NASA CONTRACTOR REPORT

MINIMUM TIME AIRCRAFT TRAJECTORIES BETWEEN TWO POINTS IN RANGE ALTITUDE SPACE

by Thomas L. Vincent and Richard G. Brusch

Prepared by
UNIVERSITY OF ARIZONA
Tucson, Ariz.
for

NATIONAL AERONAUTICS AND SPACE ADMINISTRATION • WASHINGTON, D. C. • OCTOBER 1966

MINIMUM TIME AIRCRAFT TRAJECTORIES BETWEEN TWO POINTS IN RANGE ALTITUDE SPACE

By Thomas L. Vincent and Richard G. Brusch

Prepared under Grant No. NsG-580 by
UNIVERSITY OF ARIZONA
Tucson, Ariz.

for

NATIONAL AERONAUTICS AND SPACE ADMINISTRATION

For sale by the Clearinghouse for Federal Scientific and Technical Information
Springfield, Virginia 22151 – Price $2.50

TABLE OF CONTENTS

LIST OF FIGURES

NOMENCLATURE

A	wing area of aircraft
C_1	constant defined on page 22
C_2	constant defined on page 22
C_D	drag coefficient
C_L	lift coefficient
D	drag, distance
D_1	length of initial vertical subarc
D_2	length of final vertical subarc
g	acceleration due to gravity, 32.2 ft/sec^2
H	Hamiltonian function defined on page 9
K	thrust/weight
$\bar{K}$	constant defined on page 21
L	lift
m	mass
r	(thrust minus drag)/weight
s	constant defined on page 21
R	thrust minus drag
t	independent variable
T	thrust
T_o	constant thrust
u	dimensionless velocity
$\bar{u}$	velocity defined on page 22
u_q	intermediate velocity defined on page 9
u_T	terminal velocity
U	control variable
v	velocity
v_r	reference velocity defined on page 3
W	weight of aircraft
x	range of coordinate
y	altitude coordinate; variable defined by equation (3.27)
Y	state variable
γ	flight path angle
η	dimensionless altitude
λ	Lagrange multiplier
ξ	dimensionless range
ρ_o	reference density
τ	dimensionless time

Subscripts

1	initial point
f	final point

Notation

A prime denotes differentiation with respect to non-dimensional time.

A "+" sign refers to conditions just after a corner.

A "-" sign refers to conditions just before a corner.

ABSTRACT

The methods of the calculus of variations are used in this paper for the analysis and solution to the problem of determining minimum time aircraft trajectories between two fixed points in range-altitude space. The analysis is confined to an aircraft of constant weight with the thrust and drag relationships given as specified functions of velocity and altitude. No constraints are imposed on the possible aircraft maneuvers.

Under these circumstances, it is shown that the nature of an optimal solution to a given point in range-altitude space falls into one of two distinctly different categories. The solution is either of a continuous nature with the resulting trajectory being smooth or the solution is of a discontinuous nature with the resulting trajectory containing corners. An analytical solution is presented for the discontinuous case.

A complete solution is obtained for the particular example of an aircraft with drag proportional to the square of velocity and constant thrust. It is shown that in this case, for a thrust to weight ratio greater than 1.5, only continuous time optimal solutions are obtained to each point in range-altitude space. However, for a thrust to weight ratio less than 1.5 both continuous and discontinuous solutions are needed to reach every point in range-altitude space. A common boundary line in range-altitude space is obtained which separates the region of points obtained using continuous solutions from the region of points obtained using the discontinuous solutions. The numerical procedure used for obtaining the continuous solutions is based on a flooding technique.

SECTION I

INTRODUCTION

The minimum time to climb problem in aircraft flight mechanics has been discussed extensively in the literature by several authors (1, 2, 3). This problem has been popular not only because it is of practical interest but also because of the fact that a relatively simple solution is possible if a basic model aircraft, assumed to be of constant weight, with thrust and drag given as specified functions of velocity and altitude, is used (i.e., an aircraft with a fixed throttle setting with no induced drag, or an aircraft with induced drag but with the additional assumption that lift is approximately equal to weight throughout the trajectory). The minimum time to climb problem is generally treated as a two point problem in velocity-altitude space. By definition the final range point for a time to climb problem is left free. Under these circumstances optimal solutions are characterized by the subarc nature of the resultant flight path.

Variations to this basic problem are made by relaxing certain assumptions about the aircraft and about conditions specified at the initial and final points. Solutions to the varied problems have been obtained by Hermann (4) using the calculus of variations.

Another problem which is seldom discussed but which is closely related to the minimum time to climb problem is the problem of determining the minimum time aircraft trajectory between two fixed points in range altitude space. By requiring that the final range be specified, the entire nature of the solution changes from that of the time to climb problem. The analysis and partial solution to the problem of determining optimal trajectories between two fixed points in range-altitude space using the calculus of variations has been previously discussed by Vincent (5). The material presented in this paper represents an extension of this work for a minimum time pay off function and is devoted to the complete analysis and solution of this problem for a specific model aircraft.

In order to make the problem of minimum time between two fixed points in range-altitude space tractable analytically, the basic model aircraft will again be assumed to be of constant weight with thrust and drag given as specified functions of altitude and velocity (induced drag will be neglected). In the ensuing analysis, solutions will be obtained for a model aircraft with very simple thrust and drag relations. By obtaining exact solutions to a simplified problem, rather than concentrating on an approximate solution to an exactly formulated problem, it is felt that the significance and physical meanings associated with the optimal solution for the aircraft operating under gravitational, thrust, lift and drag forces can be more readily understood and exploited.

Flight trajectories which satisfy the necessary optimizing conditions as set forth in the next section will be referred to as optimal trajectories.

SECTION II

THE TWO POINT MINIMUM TIME PROBLEM

Equations of Constraint

The model aircraft and environment. - The analysis of the time-optimal performance for an aircraft will be confined to a vehicle assumed to operate in a plane under the forces as shown below.

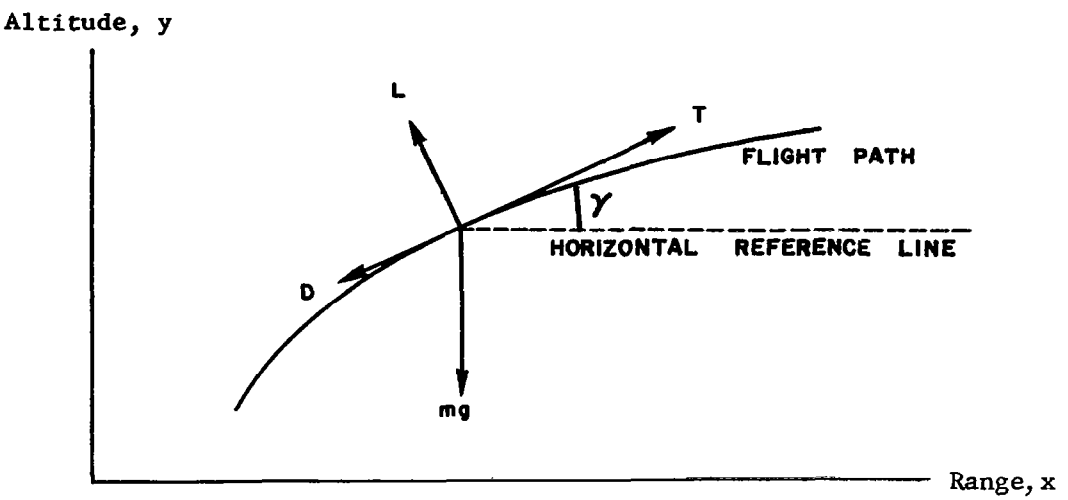

FIGURE 2.1 - APPLIED FORCES

Where:

T = thrust. The thrust force will be assumed to act in the direction of the flight path. For the purpose of analysis, the throttle setting is assumed to be fixed. Therefore, thrust will be represented as a function of velocity, v, and altitude, y. The illustrative example solutions given in Sections III and IV are obtained for thrust equal to a constant.

D = Drag. The drag force will be assumed to act opposite in direction to the inertial velocity vector, v (no relative wind). For the purpose of analysis, induced drag will be neglected. Drag will be represented as a function of velocity and altitude only. The illustrative example solutions given in Sections III and IV are obtained for drag proportional to the square of velocity.

L = Lift. The lift force will be assumed to act perpendicular to the flight path (no relative wind). No bounds will be put on the values of lift needed to fly any given trajectory. By assuming the lift to be unbounded, no analytical representation of the lift force will be needed for analysis.

mg = weight of the aircraft. The gravitational force will be assumed to act perpendicular to the horizontal reference line. The weight of the aircraft will be assumed constant in the analysis.

For a high speed aircraft, the drag and thrust would be expressed more properly in terms of Mach number. However, for simplification in order to make the comparison between high speed and low speed flight more direct, the atmosphere will be assumed to be isothermal. In this case, drag and thrust become velocity dependent for both high and low speed flight.

The non-dimensional equations of motion. - Let $T(v,y) - D(v,y) = R(v,y)$. Then the equations of motion in the tangential and normal directions may be written from Figure 2.1 as follows:

$$m\dot{v} = R(v,y) - mg \sin \gamma, \tag{2.1}$$

$$mv\dot{\gamma} = L - mg \cos \gamma, \tag{2.2}$$

with the following kinematical relations applicable between the range-altitude variables,

$$\dot{x} = v \cos \gamma, \tag{2.3}$$

$$\dot{y} = v \sin \gamma. \tag{2.4}$$

These four equations are written using the assumptions already listed, and represent dynamic bounds on the possible motion of the aircraft. Since no constraints or bounds are to be imposed on the lift, and since lift is not contained in equations (2.1), (2.3), and (2.4), then equation (2.2) is uncoupled from the other equations and may be dropped in the ensuing analysis. Equation (2.2) will be used to evaluate lift requirements once an optimal trajectory is determined.

With the assumption that the mass is constant, the remaining three equations contain four dependent variables, x, y, v, and γ so that one degree of freedom remains for control. In this case the control variable is γ and the three state variables are x, y, and v. No further constraints will be imposed on the aircraft.

In order to compare minimum time performance between various aircraft, the above equations will be put into dimensionless form. If a reference velocity is defined by the velocity of an aircraft in steady level flight at $C_L = 1$ and given by

$$v_r^2 = \frac{2\,mg}{\rho_o A}, \tag{2.5}$$

where ρ_o = sea level or any reference density,

and A = wing area of the aircraft,
then the following non-dimensional parameters may be defined:

$$\text{non-dimensional velocity} \qquad u = v/v_r, \tag{2.6}$$

$$\text{non-dimensional range} \qquad \xi = gx/v_r^2, \tag{2.7}$$

$$\text{non-dimensional altitude} \qquad \eta = gy/v_r^2, \tag{2.8}$$

$$\text{non-dimensional time} \qquad \tau = gt/v_r, \tag{2.9}$$

$$\text{non-dimensional T-D} \qquad r(u,\xi) = R/mg. \tag{2.10}$$

In terms of these dimensionless variables equations (2.1), (2.3) and (2.4) become

$$u' = r(u,\xi) - \sin\gamma, \tag{2.11}$$

$$\xi' = u\cos\gamma, \tag{2.12}$$

$$\eta' = u\sin\gamma. \tag{2.13}$$

The prime denotes differentiation with respect to the non-dimensional time, τ.

The Necessary Optimal Conditions

The Problem of Bolza. - A minimum time trajectory subject to the constraints given by equations (2.11) - (2.13) represents a special case of the problem of Bolza from the calculus of variations. The solution may be obtained from the optimizing conditions as given by this theory which are briefly summarized below.

A problem of Bolza is one which minimizes a sum of the form

$$z(Y_{i1},Y_{if},t_1,t_f) + \int_{t_1}^{t_f} f(Y_i,U_k,t)\,dt, \qquad \begin{matrix} i = 1 \ldots n \\ k = 1 \ldots m \end{matrix} \tag{2.14}$$

subject to differential equations as constraints. For problems in flight mechanics constraints usually can be expressed in the form

$$\frac{dY_i}{dt} = \Phi_i(Y_i \ldots Y_n, U_k, t), \tag{2.15}$$

where Y_i represents n state variables and U_k represents m control variables,

and t represents the independent variable. By forming the Hamiltonian function,

$$H = \lambda_i \Phi_i - f, \tag{2.16}$$

the optimizing conditions from the calculus of variations for the problem of Bolza may be written as follows:

State Variable Euler Equations: $\frac{\partial H}{\partial Y_i} + \frac{d\lambda_i}{dt} = 0.$ (2.17)

Control Variable Euler Equations: $\frac{\partial H}{\partial U_k} = 0.$ (2.18)

First integral of Euler Equations: $\frac{d H}{dt} = \frac{\partial H}{\partial t}.$ (2.19)

Transversality condition: $dz + \left[- H dt + \lambda_i \, dY_i \right]_1^f = 0.$ (2.20)

Weierstrass condition: $H_{optimal} > H_{non\text{-}optimal.}$ or $\frac{\partial^2 H}{\partial U_k^2} < 0$ (2.21)

Corner conditions: $\left[- H dt + \lambda_i \, dY_i \right]_-^+ = 0.$ (2.22)

Application of the theory. - The above conditions may be applied directly to the minimum time problem by first setting $z = 0$ and $f = 1$. Then with the constraint equations given by equations (2.11) - (2.13), the Hamiltonian as defined by equation (2.16) becomes

$$H = \lambda_u (r - \sin \gamma) + \lambda_\xi (u \cos \gamma) + \lambda_\eta (u \sin \gamma) - 1. \tag{2.23}$$

The optimizing conditions in terms of this H function reduce to the following,

ξ Euler: $\lambda_\xi' = 0,$ (2.24)

η Euler: $\lambda_u \frac{\partial r}{\partial \eta} + \lambda_\eta' = 0,$ (2.25)

u Euler: $\lambda_u \frac{\partial r}{\partial u} + \lambda_\xi \cos \gamma + \lambda_\eta \sin \gamma + \lambda_u' = 0,$ (2.26)

γ Euler: $- \lambda_u \cos \gamma - \lambda_\xi u \sin \gamma + \lambda_\eta u \cos \gamma = 0,$ (2.27)

1st integral: $H = \text{constant},$ (2.28)

$$\text{Trans:} \quad \left[- H \, d\tau + \lambda_\xi \, d\xi + \lambda_\eta \, d\eta + \lambda_u \, du \right]_1^f = 0, \tag{2.29}$$

$$\text{Weier:} \quad \lambda_u \sin \gamma - \lambda_\xi \, u \cos \gamma - \lambda_\eta \, u \sin \gamma < 0, \tag{2.30}$$

$$\text{Corner:} \quad \left[- H \, d\tau + \lambda_\xi \, d\xi + \lambda_\eta \, d\eta + \lambda_u \, du \right]_-^+ = 0. \tag{2.31}$$

A minimum time problem between two points in range-altitude space is one in which the final time is left free and the initial and final values of the ξ and η coordinates are specified. The initial value of the velocity is generally specified and the final value may or may not be fixed. For the purpose of analysis, the initial value of the velocity will be assumed to be given and the final value will be left free. Under these conditions the transversality condition yields the following information,

$$H_f = 0, \tag{2.32}$$

$$\lambda_{uf} = 0. \tag{2.33}$$

Since the Hamiltonian is a constant, equation (2.32) yields $H = 0$ throughout the trajectory. Hence equation (2.28) may be written as

$$\lambda_u (r - \sin \gamma) + \lambda_\xi \, u \cos \gamma + \lambda_\eta \, u \sin \gamma = 1. \tag{2.34}$$

Equations (2.24) - (2.27) and (2.34) may now be combined into a single differential equation, the solution of which determines the optimal control. To obtain this expression the control equation (2.27) is solved for the control variable γ,

$$\lambda_\xi \tan \gamma = \lambda_\eta - \frac{\lambda_u}{u}, \quad (\cos \gamma \neq 0) \tag{2.35}$$

and differentiated with respect to the variable τ (noting from equation (2.24) that $\lambda_\xi' = 0$), to give

$$\lambda_\xi \sec^2 \gamma \, \gamma' = \lambda_\eta' - (u \lambda_u' - \lambda_u u')/u^2. \tag{2.36}$$

The derivatives on the right hand side of equation (2.36) are eliminated by substituting the remaining Euler equations (2.25) and (2.26) and the equation of constraint (2.11) into equation (2.36) to give,

$$\lambda_\xi \sec^2 \gamma \, \gamma' = \lambda_u \left[\frac{1}{u} \frac{\partial r}{\partial u} - \frac{\partial r}{\partial \eta} \right] + \frac{1}{u^2} \left[\lambda_\xi \, u \cos \gamma + \lambda_\eta \, u \sin \gamma + \lambda_u (r - \sin \gamma) \right] . \tag{2.37}$$

The last term in brackets is equal to unity according to equation (2.34). Equations (2.27) and (2.34) may be combined to give

$$\lambda_u r = 1 - \lambda_\xi u \sec \gamma. \tag{2.38}$$

Hence if $r \neq 0$, equation (2.38) may be solved for λ_u and substituted into equation (2.37)

$$\lambda_\xi \sec^2\gamma \, \gamma' = \frac{1}{r}(1 - \lambda_\xi u \sec \gamma)\left[\frac{1}{u}\frac{\partial r}{\partial u} - \frac{\partial r}{\partial \eta}\right] + \frac{1}{u^2}. \tag{2.39}$$

If $\lambda_\xi \neq 0$, this equation may be reduced to the following expression,

$$\gamma' = \frac{\cos\gamma}{u}\left[\frac{1}{r}\left(u\frac{\partial r}{\partial u} - u^2\frac{\partial r}{\partial \eta}\right)\left(\frac{\cos\gamma}{\lambda_\xi u} - 1\right) + \frac{\cos\gamma}{\lambda_\xi u}\right]. \tag{2.40}$$

This single differential equation which is valid when $r \neq 0$ and $\lambda_\xi \neq 0$ contains all of the Euler equations, so that its solution in conjunction with the equations of constraint (2.11) - (2.13), the transversality condition (2.33), the Weierstrass condition equation (2.30) and the corner conditions (2.31) will yield a minimum time trajectory between two points in ξ - η space. The transversality condition, $\lambda_u = 0$, may be used to evaluate λ_ξ by setting the left hand side of equation (2.38) to zero to yield

$$\lambda_\xi = \frac{\cos\gamma_f}{u_f}, \tag{2.41}$$

The Weierstrass condition may be simplified by substituting equation (2.35) into equation (2.30) to obtain

$$\lambda_\xi u \sec\gamma > 0. \tag{2.42}$$

Thus sec γ must maintain the same sign as λ_ξ throughout the trajectory. If an end point is chosen to the right of the initial point, then some portion of a trajectory joining these two points must have a positive flight path angle γ. Since λ_ξ has a constant sign throughout, it is concluded that if $\lambda_\xi \neq 0$ then λ_ξ must be positive (thus the flight path angle must also be positive throughout). If equality can occur in equation (2.42) then the minimizing arc may have a corner at such a point. Equality can occur only if $\lambda_\xi = 0$ or $u = 0$. The possibility of $u = 0$ along a minimum time trajectory is physically inconsistent and will not be considered. Since λ_ξ is a constant throughout the trajectory it is either identically zero or never zero. Hence it is concluded that a trajectory between two points will either be definitely continuous throughout ($\lambda_\xi \neq 0$) or possibly discontinuous ($\lambda_\xi = 0$).

Continuous solutions ($\lambda_\xi \neq 0$). - If $\lambda_\xi \neq 0$, then the optimal trajectory is determined from the solution to equations (2.11), (2.12), (2.13), (2.40), and (2.41) summarized for convenience below. The corner condition equation (2.31) is not needed.

$$u' = r - \sin\gamma, \tag{2.11}$$

$$\xi' = u\cos\gamma, \tag{2.12}$$

$$\eta' = u\sin\gamma, \tag{2.13}$$

$$\gamma' = \frac{\cos\gamma}{u}\left[\frac{1}{r}\left(u\frac{\partial r}{\partial u} - u^2\frac{\partial r}{\partial \eta}\right)\left(\frac{\cos\gamma}{\lambda_\xi u} - 1\right) + \frac{\cos\gamma}{\lambda_\xi u}\right], \quad (r \neq 0) \tag{2.40}$$

$$\lambda_\xi = \frac{\cos\gamma_2}{u_2}. \tag{2.41}$$

Equation (2.40) is not valid whenever $r = 0$. Under these circumstances, equation (2.38) which reduces to

$$\frac{\cos\gamma}{u} = \lambda_\xi, \quad (r = 0) \tag{2.43}$$

may be used as the optimizing condition in place of equation (2.40). Under the special case of $r \equiv 0$, equations (2.11), (2.12), (2.13), (2.41), and (2.43) may be solved analytically to obtain a cycloid trajectory. This is the solution to the well-known brachistochrone problem.

Analysis and solution to equations (2.11) - (2.43) ($\lambda_\xi \neq 0$) are contained in Chapter III.

Discontinuous solutions ($\lambda_\xi = 0$). - If $\lambda_\xi = 0$, the resulting solution to the optimizing conditions may be discontinuous. In this case the optimizing conditions (2.24), (2.25), (2.26), (2.27), (2.34), (2.33), and (2.31) reduce to

$$\xi \text{ Euler:} \quad \lambda_\xi = 0, \tag{2.44}$$

$$\eta \text{ Euler:} \quad \lambda_u\frac{\partial r}{\partial \eta} + \lambda_\eta' = 0, \tag{2.45}$$

$$u \text{ Euler:} \quad \lambda_u\frac{\partial r}{\partial u} + \lambda_\eta\sin\gamma + \lambda_u' = 0, \tag{2.46}$$

$$\gamma \text{ Euler:} \quad -\lambda_u\cos\gamma + \lambda_\eta u\cos\gamma = 0, \tag{2.47}$$

$$\text{1st integral:} \quad \lambda_u(r - \sin\gamma) + \lambda_\eta u\sin\gamma = 1, \tag{2.48}$$

$$\text{Trans:} \quad \lambda_u = 0, \tag{2.49}$$

$$\text{Corner:} \quad H^- = H^+,\ \lambda_\eta^- = \lambda_\eta^+,\ \lambda_u^- = \lambda_u^+. \tag{2.50}$$

From equation (2.47) the possible subarc solution $\cos\gamma = 0$ is obtained. If $\cos\gamma \neq 0$, then equation (2.47) may be written as

$$\lambda_\eta u = \lambda_u. \tag{2.51}$$

Equations (2.45), (2.46), (2.47) and (2.51) may now be combined into a single optimizing condition. To obtain this expression, equation (2.51) is differentiated with respect to τ to give

$$\lambda_\eta' u + \lambda_\eta u' = \lambda_\eta'. \tag{2.52}$$

The derivatives are eliminated by substituting equations (2.45), (2.46), and (2.11) for λ_η', λ_u', and u' to give

$$\lambda_u \left[\frac{\partial r}{\partial u} - u \frac{\partial r}{\partial \eta} \right] + r \lambda_\eta = 0. \tag{2.53}$$

Substituting (2.51) into (2.53) and dividing by λ_η ($\lambda_\eta \neq 0$) results in

$$u \frac{\partial r}{\partial u} - u^2 \frac{\partial r}{\partial \eta} + r = 0, \tag{2.54}$$

or

$$\frac{\partial (ur)}{\partial u} - u \frac{\partial (ur)}{\partial \eta} = 0. \tag{2.55}$$

It is interesting to note that equation (2.55) is identical with the well-known climb program for the minimum time to climb problem (2).

Joining of subarc solutions. - Trajectories in which $\lambda_\xi = 0$ throughout can in general be composed of four types of subarcs; vertical dives and climbs given by

$$\cos \gamma = 0. \tag{2.56}$$

and intermediate subarcs given by the solution to equation (2.55)

$$u_q = u_q(\eta). \tag{2.57}$$

Trajectories resulting from following the velocity-altitude program given by equation (2.57) are obtained by substituting this relationship back into the equations of motion (2.11) - (2.13) and solving for the flight path. The resulting trajectories are symmetrical and may proceed either to the right or left. The choice of optimal trajectories at a corner point is summarized in Figure 2.2.

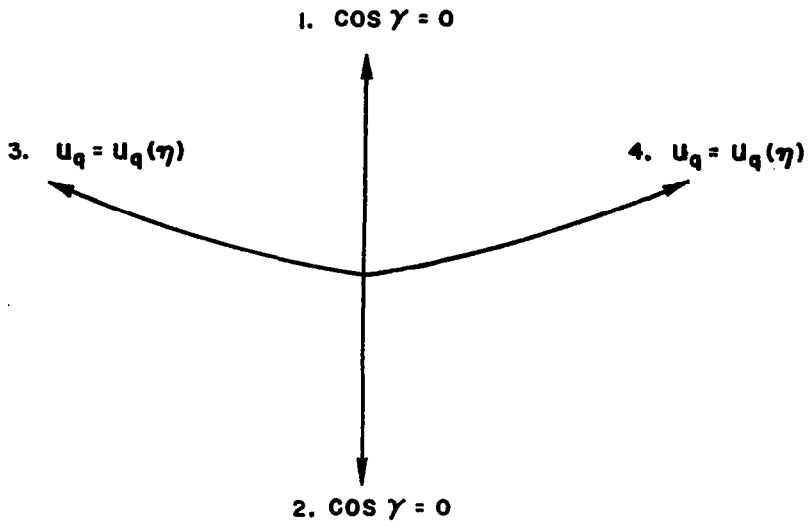

FIGURE 2.2 - CHOICE OF OPTIMAL TRAJECTORIES

The order and restrictions under which these trajectories are joined are determined from the transversality and corner conditions. There are basically three different types of corners.

Type 1. Arcs 1 or 2 joined with arcs 3 or 4
Type 2. Arcs 3 joined with arcs 4
Type 3. Arcs 1 joined with arcs 2

Corners of type 1. - The corner conditions require that the Lagrange multipliers λ_u and λ_η be continuous. In addition, all the state variables are continuous at the corners. Hence, no special notation will be used to denote these variables just before and after the corners. The corner condition on the Hamiltonian given by equation (2.50) thus reduces to the following.

Arcs 1 with 3 or 4:
$$\lambda_u(r - 1) + \lambda_\eta u - 1 = \lambda_u(r - \sin\gamma_-) + \lambda_\eta(u \sin\gamma_-) - 1. \tag{2.58}$$

Arcs 2 with 3 or 4:
$$\lambda_u(r + 1) - \lambda_\eta u - 1 = \lambda_u(r - \sin\gamma_-) + \lambda_\eta(u \sin\gamma_-) - 1. \tag{2.59}$$

Along subarcs of the type 3 or 4 the Lagrange multiplier λ_η and λ_u are related by equation (2.51). Substituting this equation into the above

reduces these equations to the following.

Arcs 1 with 3 or 4: $\lambda_\eta u(r - 1) = \lambda_u(r - 1)$. (2.60)

Arcs 2 with 3 or 4: $\lambda_\eta u(r + 1) = \lambda_u(r + 1)$. (2.61)

From equation (2.11) it is seen that the quantities $(r - 1) = 0$ and $(r + 1) = 0$ correspond to terminal climb velocity and terminal dive velocity, respectively. Hence these conditions may be ruled out as a possibility to satisfy equation (2.60) and equation (2.61), unless the solution to equation (2.55) yields the terminal climb or dive as an optimal solution (the velocity at the corner must be continuous). Discarding the possibility of $(r - 1) = 0$ and $(r + 1) = 0$, both equation (2.60) and equation (2.61) yield the same result.

$$\lambda_\eta u = \lambda_u. \tag{2.62}$$

Equation (2.62) is identical with equation (2.51). This latter equation was used in conjunction with the Euler equations to yield the velocity program $u = u_q(\eta)$. Thus the velocity at which a switch may occur is equal to the velocity along the intermediate subarc $u_q(\eta)$. Hence it is concluded that a vertical dive or climb may be optimally joined to the intermediate subarc when the velocity in the vertical dive or climb is equal to $u_q(\eta)$. Since the velocity program in a vertical dive or climb is generally either increasing or decreasing, there is usually only one point in a given dive or climb in which a switch may take place. It is also apparent from these conditions that the intermediate subarc may be left at any point to optimally join a vertical dive or climb.

Corners of type 2. - The corner condition on the Hamiltonian function in this case is given by

Arcs 3 with 4: $\lambda_u(r - \sin\gamma_-) + \lambda_\eta(u \sin\gamma_-) - 1 =$

$$\lambda_u(r - \sin\gamma_+) + \lambda_\eta(u \sin\gamma_+) - 1. \tag{2.63}$$

The Lagrange multipliers λ_u and λ_η are related by equation (2.51) on either side of the corner. Substituting equation (2.51) into the above reduces equation (2.63) to an identity. It is concluded that an intermediate subarc to the right may be optimally joined with an intermediate subarc to the left at any point, or vice versa.

Corners of type 3. - The corner condition on the Hamiltonian function in this case is given by

Arcs 1 with 2: $\lambda_u(r - 1) + \lambda_\eta u - 1 = \lambda_u(r + 1) - \lambda_\eta u - 1,$ (2.64)

or $$2\left[\lambda_u - \lambda_\eta u\right] = 0. \tag{2.65}$$

Using the same arguments as before, it is easy to show from equation (2.65)

that a vertical dive may be optimally joined to a vertical climb when $u = \dot{u}_q(\eta)$ and vice versa.

Optimal arrangement of trajectories. - From the preceding discussion it was observed that a switch from one optimal subarc to another can be made only when $u = u_q(\eta)$. Along vertical subarcs, velocity is generally an increasing or decreasing function of time and along intermediate subarcs $u = u_q(\eta)$. Thus once an aircraft switches to a vertical subarc from any other subarc, it cannot optimally switch off of the vertical subarc but must remain on that trajectory thereafter. However, an aircraft may optimally switch from one intermediate subarc to another any number of times. Figure 2.3 illustrates these possibilities.

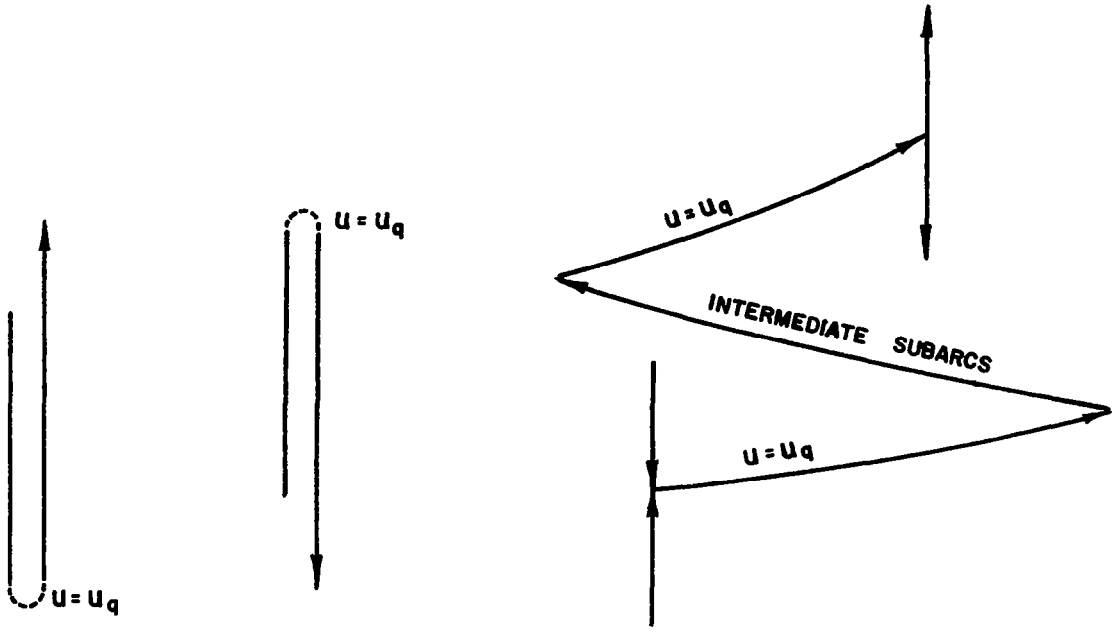

FIGURE 2.3 - OPTIMAL SWITCHING

Unless the initial specified velocity is given by $u = u_q(\eta)$ it is concluded that flight trajectories in which the $\lambda_\xi = 0$ solution is valid will start with an initial dive or climb and remain in vertical flight until the velocity $u = u_q(\eta)$ is obtained. At this point a switch is made to the intermediate trajectory (except for an endpoint directly above the origin).

When the transversality condition, $\lambda_{uf} = 0$, is substituted into equations (2.47) and (2.48) the following results are obtained:

$$\lambda_{\eta f} u \cos \gamma_f = 0, \tag{2.66}$$

$$\lambda_{\eta f} u \sin \gamma_f = 1. \tag{2.67}$$

The only way both of these equations can be satisfied is for $\cos \gamma_f = 0$. Thus the final subarc must be a vertical trajectory which from equation (2.67) must pass through the final specified endpoint with the following velocity.

$$u_f = \pm \frac{1}{\lambda_{\eta f}} \tag{2.68}$$

where the plus sign corresponds to a vertical climb and the minus sign corresponds to a vertical dive. Hence the sign of $\lambda_{\eta f}$ will determine whether the proper final trajectory is a vertical dive or climb. This latter condition also dictates the vertical distance increment between the final endpoint and the last switch point. Figure 2.4 illustrates a typical trajectory between two points for the case of $\lambda_\xi = 0$

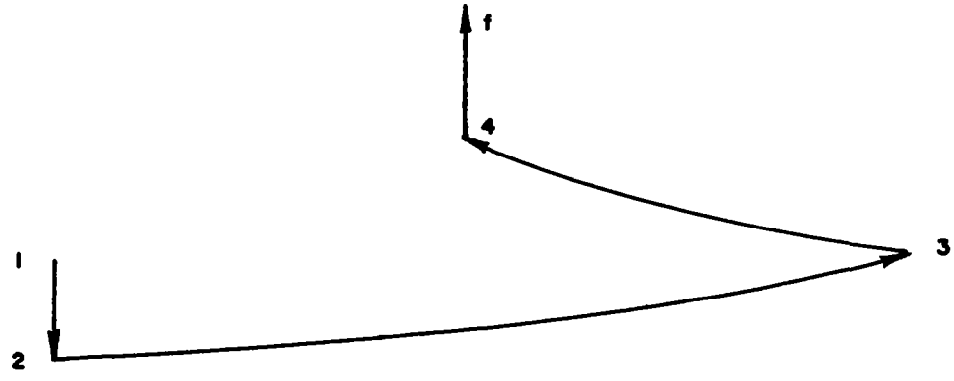

FIGURE 2.4 - TYPICAL TRAJECTORY WITH $\lambda_\xi = 0$

The value of $\lambda_{\eta f}$ must in general be obtained from the integration of the Euler equations. If, however, the change in r due to altitude variation over this final subarc can be considered to be small, then from equation (2.45) the result is obtained that λ_η = constant. Thus in this case

$$\lambda_{\eta f} = \lambda_{\eta 4}. \qquad \text{(Fig. 2.4)} \tag{2.69}$$

The value of λ_η anywhere along the intermediate trajectory may be obtained by substituting equation (2.51) into equation (2.48) to obtain

$$\lambda_\eta = \frac{1}{u\, r}. \tag{2.70}$$

In particular

$$\lambda_{\eta 4} = \frac{1}{u_{q4}\, r_{q4}} \tag{2.71}$$

The total solution. - It was concluded in the preceding discussion that a minimum time trajectory to a given point will either be completely

continuous or discontinuous as shown in Figure 2.4. The particular points in state space which are obtained with either continuous or discontinuous solutions will of course depend upon the performance characteristics assigned to a particular model aircraft and upon the choice of initial conditions. For a given model aircraft the initial conditions alone should dictate the location of the regions in which continuous or discontinuous solutions exist. Logically, these two regions should not overlap. The boundary between the two regions can be determined either by finding the limiting cases for continuous solutions or by finding the limiting cases for discontinuous solutions. This latter procedure will be used in the next section since it is easier. The minimum time solution for a particular model aircraft will be determined throughout state space in sections III and IV.

SECTION III

DISCONTINUOUS SOLUTIONS

The Optimizing Conditions

Supplementary comments. - In the preceding analysis thrust and drag were assumed to be expressible as functions of altitude and velocity. This is a limiting assumption since induced drag cannot realistically be accounted for under such a restriction. However, induced drag is usually small for high speed flight and often can be neglected. A much more serious disadvantage lies in the fact that the results of Section II cannot be implemented until some mathematical functional form is chosen for the thrust and drag. A simple yet accurate mathematical representation for the thrust and drag in terms of altitude and velocity is not possible for the spectrum of flight regimes covered by high performance aircraft. Experimentally accurate thrust and drag variations with altitude and velocity are available from wind tunnel data and engine test curves. But such data, in general, cannot be expressed in terms of simple analytical equations.

For the purpose of obtaining the major effects of thrust and drag on the form of an optimal trajectory the detailed variations in engine and drag data will be neglected. In the analysis which follows, thrust and drag will be expressed by the simplest physically consistent functional form that can possibly be assumed and yet maintain the gross effects of these forces. For the model aircraft to be considered, the thrust will be assumed to be constant

$$T = T_o. \tag{3.1}$$

This assumption is accurate for a rocket engine or for a turbojet engine operating over a limited range of altitude and velocity. The drag will be expressed as

$$D = \frac{1}{2} \rho_o A C_D v^2. \tag{3.2}$$

With the density ρ_o, assumed constant, this relationship is reasonably accurate for an aircraft operating with limited variations in altitude and velocity.

In the terms of the nondimensional velocity, the drag may be written as

$$D = C_D u^2 mg. \tag{3.3}$$

With the mass of the aircraft assumed constant the non-dimensional thrust minus drag may be written as

$$r = \frac{T - D}{mg} = K - C_D u^2, \tag{3.4}$$

where K is the constant thrust to weight ratio. With this functional relationship for r the equations of constraint which must be satisfied for both continuous and discontinuous trajectories become

$$u' = K - C_D u^2 - \sin \gamma, \tag{3.5}$$

$$\xi' = u \cos \gamma, \tag{3.6}$$

$$\eta' = u \sin \gamma. \tag{3.7}$$

With these assumptions the optimizing conditions (2.55) and (2.56) for discontinuous solutions become

$$u_q = \sqrt{\frac{K}{3C_D}}, \quad (\cos \neq 0) \tag{3.8}$$

or

$$\cos \gamma = 0. \tag{3.9}$$

The end point, condition (2.68) may be evaluated explicitly since λ_η under these assumptions is constant. Evaluation of equation (2.68) along the intermediate trajectory by means of equation (2.71) gives

$$u_f = \frac{2}{3} K \sqrt{\frac{K}{3C_D}}. \tag{3.10}$$

Analysis

The subarc solutions. - For the particular case under consideration, the intermediate trajectory corresponds to a steady flight situation. With u_q given by equation (3.8), the equation of motion in the tangential direction given by equation (3.5) reduces to

$$\sin \gamma = \frac{2}{3} K. \tag{3.11}$$

Since this equation has no solution for $K > 3/2$, it is concluded that discontinuous solutions with steady intermediate arcs will exist only for values of the thrust to weight ratio $K < 3/2$.

It has been shown that the final subarc must correspond to vertical flight and that the velocity at the final point must correspond to

$$u_f = \frac{2}{3} K u_q.$$

Under this circumstance with $K < \frac{3}{2}$ it is easy to show that the final subarc is a climbing subarc. This conclusion is made from the following considerations:

1. The terminal velocity in a vertical dive or climb, obtained by setting $u' = 0$ and $\sin \gamma = \pm 1$ in equation (3.5), is given by

$$u_{Tclimb} = \sqrt{\frac{K - 1}{C_D}} \tag{3.12}$$

or

$$u_{Tdive} = \sqrt{\frac{K + 1}{C_D}} \tag{3.13}$$

2. The velocity on the intermediate steady subarc is given by

$$u_q = \sqrt{\frac{K}{3C_D}}. \tag{3.14}$$

3. The initial acceleration as given by equation (3.5) upon leaving the intermediate steady subarc to a dive or climb is given by

$$u'_{lclimb} = \frac{2}{3} K - 1, \tag{3.15}$$

or

$$u'_{ldive} = \frac{2}{3} K + 1. \tag{3.16}$$

If $K < \frac{3}{2}$, then equations (3.12) - (3.14) may be used to show that

$$u_{Tclimb} < u_f < u_q, \tag{3.17}$$

$$u_{Tdive} > u_q, \tag{3.18}$$

$$u'_{lclimb} < 0, \tag{3.19}$$

and

$$u'_{ldive} > 0. \tag{3.20}$$

Thus in a climb the velocity will decrease from u_q to the terminal velocity, whereas, in a dive the velocity will increase from u_q to the terminal velocity. Since the optimal final velocity, u_f, is less than u_q but greater than $u_{T_{climb}}$, the only possible vertical subarc is a climbing one.

If $K = \frac{3}{2}$ the intermediate trajectory is identical with the final vertical subarc since by equation (3.11) $\gamma = \pm 90^\circ$. But since

$$u_{T_{climb}} = \sqrt{\frac{1}{2C_D}} = u_q,$$

it is concluded that in this case the intermediate/final subarc is a vertical climb.

It is interesting to note that by substitution of equation (3.8) and (3.11) into equation (3.7), the following expression for the rate of climb of the aircraft along the steady intermediate trajectory is obtained,

$$\eta' = \frac{2}{3} K \sqrt{\frac{K}{3C_D}}, \tag{3.21}$$

which is identical to the optimal terminal velocity. For this problem equation (3.21) represents the maximum continuous rate of climb for the aircraft. The fact that the optimal final velocity is equal to the maximum rate of climb is perhaps intuitively obvious. If the velocity on the final vertical climb dropped below the maximum continuous rate of climb, then a better trajectory could be obtained by flying along the steady intermediate trajectory.

At the start of any trajectory it is assumed that the initial point and velocity will be specified. There are three possibilities for the initial velocity which will dictate the nature of the initial subarc. These possibilities are

$$u_1 = u_q, \tag{3.22}$$

$$u_1 > u_q, \tag{3.23}$$

and

$$u_1 < u_q. \tag{3.24}$$

Trajectories with $u_1 = u_q$. - From equations (3.19) and (3.20) and equation (3.5) it is seen that if the aircraft starts off either in a vertical dive or climb the velocity either increases or decreases with time. Hence a switch can never be made from these trajectories. Only on the climbing trajectory can the final velocity condition $u_f = \frac{2}{3} K u_q$ be met. This condition will be met only at one point directly overhead. The other possible trajectory in this case is to initially embark on the steady intermediate trajectory either to the right or left. Once on this trajectory a switch can be made from a right running trajectory to a left running trajectory at

any point, or vice versa, but it is obvious that only one switch can be made to vertical trajectory and this must be to a vertical climbing trajectory which intersects the final endpoint with a velocity $u_f = \frac{2}{3} K u_q$. By examining all possible solutions in this case it is readily seen as shown in Figure 3.1 that there is a boundary above which solutions of this nature are possible ($\lambda_\xi = 0$)

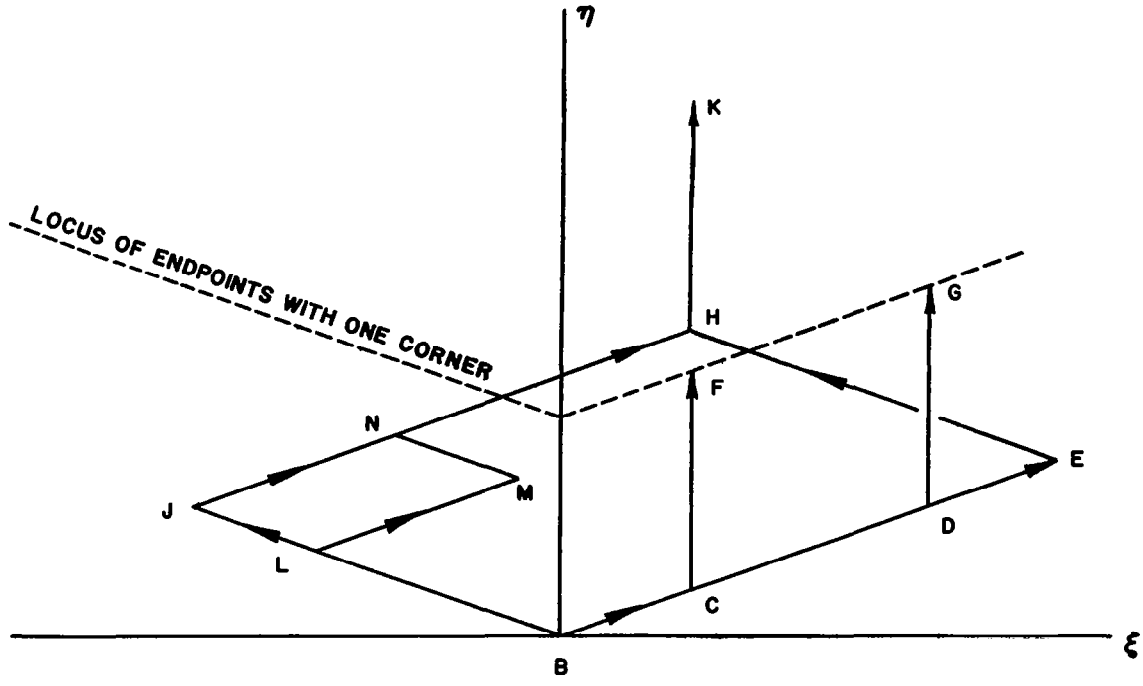

FIGURE 3.1 SOME TYPICAL TRAJECTORIES WITH $u_1 = u_q$ ($\lambda_\xi = 0$)

The boundary in this case corresponds to the locus of endpoints of trajectories with just one corner. There is only one possible trajectory to each point on this locus. For example, trajectories BCF and BDG represent two typical trajectories. If an endpoint lies above this line, then there is more than one way of optimally reaching that endpoint. There are two ways of reaching the point K with trajectories with two corners; these are illustrated by trajectories BEHK and BJHK in Figure 3.1. If trajectories of more than two corners to the point K are considered, then the possible ways of obtaining this point become infinite. Trajectory BLMNHK illustrates an example trajectory with more than two corners. All of the trajectories to the point K are confined to lie within the parallelogram BEHJ.

Trajectories with $u_1 > u_q$. - It is evident that in this case the initial trajectory must be a vertical climb, since if a vertical dive were used, the velocity would either monotonically decrease or increase to the terminal

velocity which according to eq (3.18) is greater than u_q. Thus the endpoint condition or a switch condition could never be met.

If a trajectory is undertaken with an initial vertical climb, the velocity will decrease from u_1 until the velocity u_q is attained. At this point a switch may be made to an intermediate trajectory and conclusions in regard to possible endpoints may be made as in the previous section. If, after the vertical climb, a switch is made to a vertical dive instead, the possibility of satisfying the condition for a switch or endpoint can never be met and hence this possibility must be discarded. If no switch is made at this point, the velocity will continue to decrease until the velocity $u_2 = \frac{2}{3} K u_q$ is obtained. At this point the trajectory must be terminated.

If all possible solutions are examined in this case a boundary of endpoints is obtained as shown in Figure (3.2)

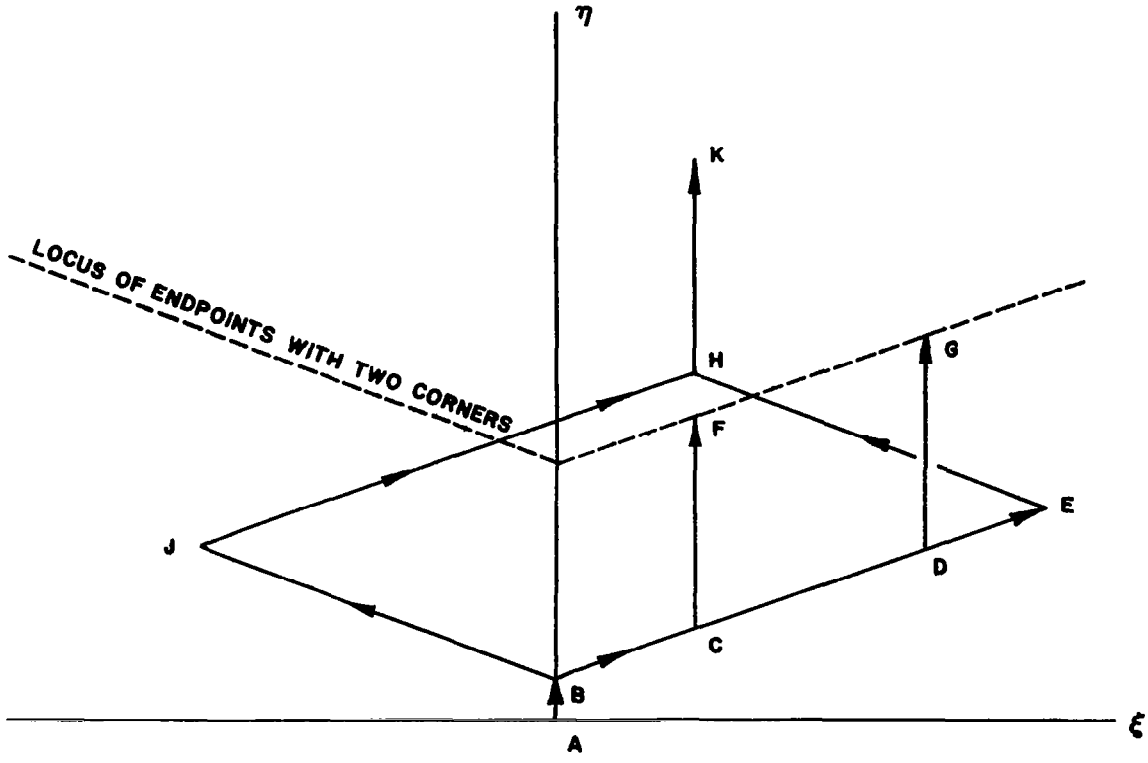

FIGURE 3.2 - SOME TYPICAL TRAJECTORIES WITH $u_1 > u_q$ ($\lambda_\xi = 0$)

The boundary in this case corresponds to the locus of endpoints to trajectories with just two corners. There is only one possible trajectory at each point on this locus. Typical trajectories to points on the locus are represented by segments ABCF & ABDG in Figure 3.2. For an endpoint above this locus there is more than one way of optimally reaching a given point. There are two ways of reaching the point K with trajectories of three corners, illustrated by segments

ABEHK and ABJHK, and an infinite number of ways of reaching the point K with trajectories of more than three corners. All trajectories to the point K lie within the parallelogram BEHJ.

Trajectories with $u_1 < u_q$. - In this case the aircraft must again start in vertical flight. It is evident that if $u_f < u_1 < u_q$, then the final condition $u_f = 2/3\ K\ u_q$ can be attained with a vertical climb. This is a possible trajectory (a continuous one) but is the only one possible starting with a vertical climb since the switching velocity u_q will never be attained by starting with climbing flight. Hence for this case a discontinuous solution must start with a vertical dive, until the velocity u_q is attained. At this point a switch must either be made to a vertical climb or to the intermediate trajectory (the endpoint condition cannot be met if the dive is continued). By examining all possible trajectories a boundary of endpoints is again attained as shown in Figure 3.3.

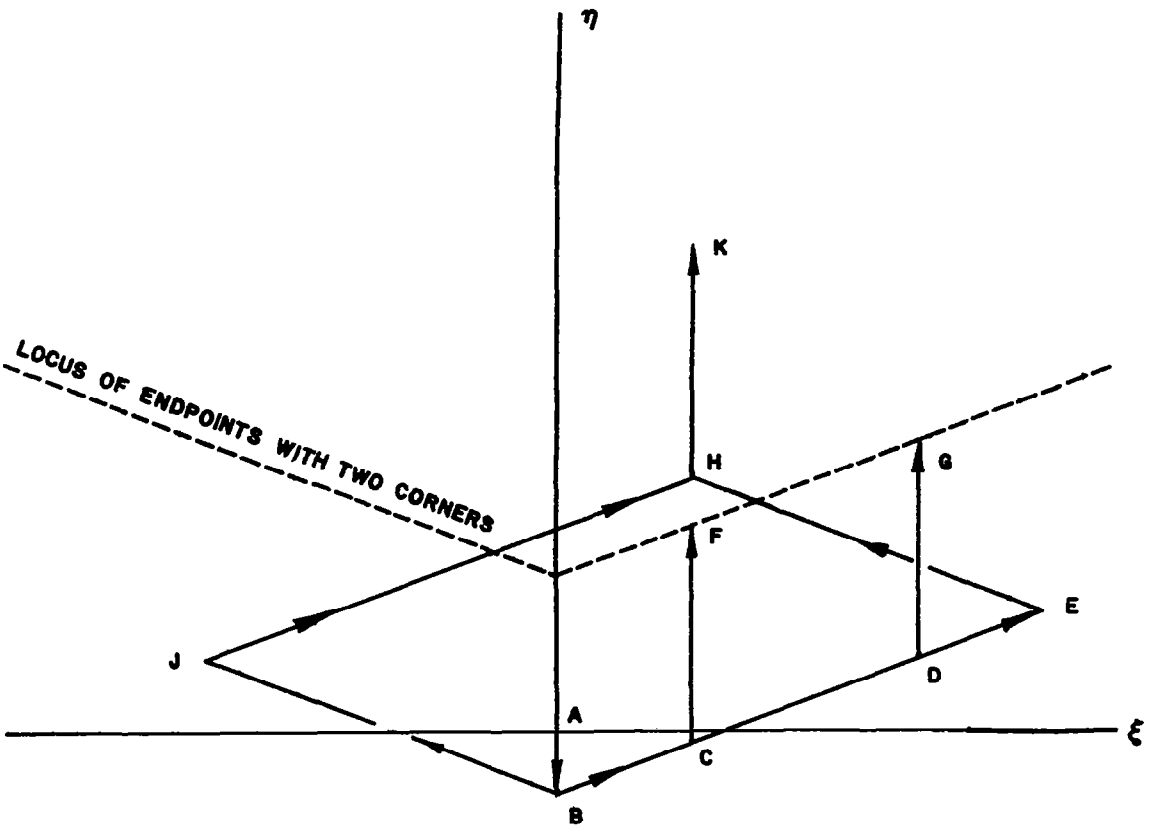

FIGURE 3.3 - SOME TYPICAL TRAJECTORIES WITH $u_1 < u_q$ ($\lambda_\xi = 0$)

Again in this case the boundary above which discontinuous solutions exist is composed of the locus of end points of trajectories with just two corners. The segments ABCF and ABDG represent typical trajectories to the endpoints F and G. There is only one trajectory to each endpoint on this boundary. Above this boundary, as before, there are two trajectories with three corners and an infinite number of trajectories with more than three corners to each endpoint. The segments ABEHK and ABJHK represent trajectories with three corners to the point K.

Location of boundary locus. - The boundary above which discontinuous solutions are possible are shown in Figures 3.1 - 3.3 for the initial conditions $u_1 = u_q$, $u_1 > u_q$ and $u_1 < u_q$. The slope of the boundary is identical withthe slope of the intermediate trajectory and hence may be determined from equation (3.11). Thus the boundary line is completely determined if its intercept with the η axis can be determined. In general this intercept point can be located by calculating the vertical distance traveled on the initial dive or climb $D_1 = AB$ (Figures 1 - 3) ($D_1 = 0$ if $u_1 = u_q$) and subtracting or adding this value for a dive or climb respectively to the distance traveled during the final climb $D_2 = CF = DG = HK$ (Figures 1 - 3).

The distances D_1 and D_2 are obtained by integrating the equations of motion with $\gamma = \pm 90^\circ$. By setting $\gamma = \pm 90^\circ$ in equations (3.5) and (3.6) the following results are obtained:

$$u' = \bar{K} - C_D u^2, \tag{3.25}$$

$$\eta' = u . \tag{3.26}$$

where $\bar{K} = K - 1$ for a climb,

and $\bar{K} = K + 1$ for a dive.

Equation (3.25) is a simple form of the Riccati equation and may be integrated to yield the velocity as a function of time by making the transformation

$$u = \frac{1}{C_D} \frac{y'}{y} \tag{3.27}$$

Changing variables in equation (3.25) by means of equation (3.27) yields

$$y'' - \bar{K} C_D y = 0. \tag{3.28}$$

The nature of the solution to equation (3.28) depends upon whether $\bar{K}$ is positive or negative. If $\bar{K} > 0$, let $s^2 = \bar{K} C_D$ and if $\bar{K} < 0$, let $s^2 = \bar{K} C_D$. Thus equation (3.28) may be written as

$$y'' - s^2 y = 0 , \qquad (\bar{K} > 0) \tag{3.29}$$

or

$$y'' + s^2 y = 0 , \qquad (\bar{K} < 0) \tag{3.30}$$

with the solutions

$$y = A_1 \sinh s\tau \quad B_1 \cosh s\tau \qquad (\bar{K} > 0) \qquad (3.31)$$

or

$$y = A_2 \sin s\tau + B_2 \cos s\tau. \qquad (\bar{K} < 0) \qquad (3.32)$$

Substituting equations (3.31) and (3.32) into equation (3.27) yields the following expressions for the velocity:

$$u = \frac{s}{C_D} \left[\frac{C_1 + \tanh s\tau}{1 + C_1 \tanh s\tau} \right] , \quad (\bar{K} > 0) \qquad (3.33)$$

or

$$u = \frac{s}{C_D} \left[\frac{C_2 - \tan s\tau}{1 + C_2 \tan s\tau} \right] . \quad (\bar{K} < 0) \qquad (3.34)$$

The constants C_1 and C_2 in equations (3.33) and (3.34) can be evaluated from the initial condition $u = u_1$, at time $t = 0$ to give

$$C_1 = C_2 = \frac{u_1 C_D}{s} . \qquad (3.35)$$

On the final arc D_2, $u_1 \equiv u_q$. The time on the final arc can be measured from zero in this case.

By defining the following quantities

$$u_T = \frac{s}{C_D} \quad \text{(terminal velocity)} , \qquad (3.36)$$

and

$$\bar{u} = u/u_T . \qquad (3.37)$$

then with the use of these definitions and equation (3.35), equations (3.33) and (3.34) become

$$\bar{u} = \frac{\bar{u}_1 + \tanh s\tau}{1 + \bar{u}_1 \tanh s\tau} , \qquad (\bar{K} > 0) \qquad (3.38)$$

and

$$\bar{u} = \frac{\bar{u}_1 - \tan s\tau}{1 + \bar{u}_1 \tan s\tau} . \qquad (\bar{K} < 0) \qquad (3.39)$$

If the above equations are now substituted into equation (3.26) and integrated with the initial condition $\eta = 0$ when $t = 0$, then the following results are obtained:

$$D = \frac{1}{C_D} \ell n \left[\frac{1 + \bar{u}_1 \tanh s\tau}{\sqrt{1 - \tanh^2 s\tau}} \right], \quad \bar{K} > 0 \qquad (3.40)$$

$$D = \frac{1}{C_D} \ell n \left[\frac{1 + \bar{u}_1 \tan s\tau}{\sqrt{1 + \tan^2 s\tau}} \right] . \quad \bar{K} < 0 \qquad (3.41)$$

In order to evaluate the distance D_1 spent on the initial vertical subarc, the time spent on the subarc may be evaluated using equations (3.38) and (3.39). By setting $\bar{u} = \bar{u}_q = \sqrt{\frac{k}{3C_D}} / \frac{s}{C_D}$ the following expressions are obtained:

$$\tanh (s\tau) = \frac{\bar{u}_1 - \bar{u}_q}{\bar{u}_1 \bar{u}_q - 1} , \quad \bar{K} > 0 \qquad (3.42)$$

$$\tan (s\tau) = \frac{\bar{u}_1 - \bar{u}_q}{\bar{u}_1 \bar{u}_q + 1} . \quad \bar{K} < 0 \qquad (3.43)$$

Substituting these results into equations (3.40) and (3.41) yields the following expressions for the distance traveled on the initial vertical subarc:

$$D_1 = \frac{1}{2C_D} \ell n \left[\frac{\bar{u}_1^2 - 1}{\bar{u}_q^2 - 1} \right], \quad \bar{K} > 0 \qquad (3.44)$$

$$D_1 = \frac{1}{2C_D} \ell n \left[\frac{\bar{u}_1^2 + 1}{\bar{u}_q^2 + 1} \right] . \quad \bar{K} < 0 \qquad (3.45)$$

In order to evaluate the distance D_2 spent on the final vertical subarc, the time spent on the subarc must first be evaluated using equations (3.38) and (3.39) by setting $\bar{u} = \frac{2k}{3} \bar{u}_q$ and $\bar{u} = \bar{u}_q$ and solving for $(s\tau)$, which gives

$$\tanh(s\tau) = \frac{\bar{u}_q \left(1 - \frac{2}{3} K \right)}{\frac{2K}{3} \bar{u}_q^2 - 1} , \quad \bar{K} > 0 \qquad (3.46)$$

$$\tan (s\tau) = \frac{\bar{u}_q \left(1 - \frac{2}{3} K \right)}{\frac{2K}{3} \bar{u}_q^2 + 1} . \quad \bar{K} < 0 \qquad (3.47)$$

Substituting these results into equations (3.40) and (3.41) yields the following expressions for the distance traveled on the final vertical subarc:

$$D_2 = \frac{1}{2C_D} \ln \left[\frac{\bar{u}_q^2 - 1}{\frac{4}{9} K^2 \bar{u}_q^{-2} - 1} \right], \qquad \bar{K} > 0 \qquad (3.48)$$

$$D_2 = \frac{1}{2C_D} \ln \left[\frac{\bar{u}_q^2 - 1}{\frac{4}{9} K^2 \bar{u}_q^{-2} + 1} \right]. \qquad \bar{K} < 0 \qquad (3.49)$$

If $\bar{K} < 0$ then the intercept point of the boundary locus with the η axis is evaluated by adding together the values of D_1 and D_2 as obtained from equations (3.45) and (3.49). If $\bar{K} > 0$, then this intercept point is evaluated by either adding the value of D_1 to D_2 or subtracting the value of D_1 from D_2 as obtained from equations (3.44) and (3.48) depending upon whether the initial arc is a vertical dive or climb.

The value of the initial velocity, u_1, the thrust to weight ratio, K, and the drag coefficient, C_D, completely determine the location of the intercept point. To determine the intercept point this information is first used to evaluate u_q from equation (3.14). If $u_1 > u_q$, the initial trajectory is a vertical climb and if $u_1 < u_q$ the initial trajectory is a vertical dive. The constant $\bar{K}$ is then evaluated from

$$\bar{K} = K - 1, \quad \text{for a climb}$$

$$\bar{K} = K + 1, \quad \text{for a dive}$$

With this information, the parameter s is then evaluated from

$$s^2 = \bar{K} C_D, \text{ if } K < 0$$

$$s^2 = -\bar{K} C_D, \text{ if } \bar{K} > 0 .$$

The terminal velocity is then evaluated from equation (3.36) so that the qualities,

$$\bar{u}_1 = u_1/u_T ,$$

and

$$\bar{u}_q = u_q/u_T ,$$

may be evaluated. Once $\bar{u}_1$ and $\bar{u}_q$ are determined the time spent or distance traveled on each of the vertical subarcs is obtained from equations (3.42)-(3.49).

SECTION IV

CONTINUOUS SOLUTIONS

Computational Procedure

Supplementary comments. - The model aircraft used in this section to determine the nature of continuous solutions will be the same as that used in Section III to determine the nature of the discontinuous solutions. Thus the controlling equations of constraint as given by equations (2.11)-(2.13) will be identical to those used in Section III, equations (3.5)-(3.7), which for convenience are again written as

$$u' = K - C_D u^2 - \sin \gamma, \tag{4.1}$$

$$\xi' = u \cos \gamma, \tag{4.2}$$

$$\eta' = u \sin \gamma. \tag{4.3}$$

The optimizing conditions for continuous trajectories as given by equations (2.40), (2.43) and (2.41) reduce to the following for an aircraft operating under the above equations of constraint.

$$\gamma' = \frac{\cos}{u} \left[\frac{2C_D u^2}{K - C_D u^2} \left(1 - \frac{\cos \gamma}{\lambda_\xi u} \right) + \frac{\cos \gamma}{\lambda_\xi u} \right] \qquad r \neq 0 \tag{4.4}$$

or

$$\frac{\cos \gamma}{u} = \lambda_\xi, \qquad r = 0 \tag{4.5}$$

where

$$\lambda_\xi = \frac{\cos \gamma_2}{u_2} \tag{4.6}$$

An optimal solution requires integration of the above set of equations. This set contains four first-order non-linear differential equations in the four variables u, ξ, η, and γ. Four constants of integration and a value for the constant λ_ξ are needed in order to completely determine a solution. As formulated, three of these constants of integrations are the specified initial conditions for the state variables u, ξ, and η. The fourth constant of integration, the initial flight path angle γ_1, is unknown.

A direct approach to solving these equations would be one in which consecutive guesses are made for both γ_1, and λ_ξ so that the equations can be repeatedly integrated until the resultant trajectory in passing through the desired endpoint satisfies equation (4.6). Such an approach, however, is not desirable from the standpoint of the difficulty of adjusting the constants γ_1 and λ_ξ to meet specified end conditions. The sensitivity of an endpoint to these parameters is a function of endpoint location. Generally speaking, the

further the endpoint is located from the initial point, the greater the sensitivity of the solution will be to adjustments in λ_ξ and γ_1. Under such circumstance, a boundary is soon reached, such that trajectories beyond this boundary cannot be obtained by using the direct approach even with an extensive digital computer system. A more detailed discussion of these difficulties plus a detailed outline of the computational procedure which was used here for the problem under consideration is given in reference 5.

Flooding technique. - In order to avoid the difficulties associated with the above mentioned direct approach to the two point boundary value problem, the so-called flooding technique may be used to generate a solution. With this technique solutions are generated by systematically varying the unknown parameters, γ_1 and λ_ξ, throughout their allowable ranges. For a given set of initial conditions equations (4.1)-(4.4) are integrated until the endpoint condition, $\lambda_\xi = \gamma_2/u_2$ $(r \neq 0)$, is met. In this way the endpoint for any set of starting conditions simply falls where it may. A manifold of optimal trajectories is generated, and the complete region of space throughout which solutions are possible can be determined.

The use of the flooding technique yields such a large number of results that the solution to all points in space may be easily visualized and areas of unusual interest quickly discovered. From this resultant manifold of solutions, the solution to a particular two point problem can at the very least be readily approximated (such an approximation may not be possible to obtain using the direct approach).

As an example of the computing procedure and method of presentation to be used in this chapter, suppose that γ_1 is set to the value of -30° and that equations (4.1)-(4.4) are integrated with several different values for λ_ξ as shown in Figure 4.1. If λ_ξ is varied in a manner such that the distance between the endpoints of any two adjacent trajectories is relatively small, then the endpoints may be joined in a continuous fashion to form a "locus of optimal endpoints." Any point on this locus can be reached optimally by starting with the given value of the initial flight path angle.

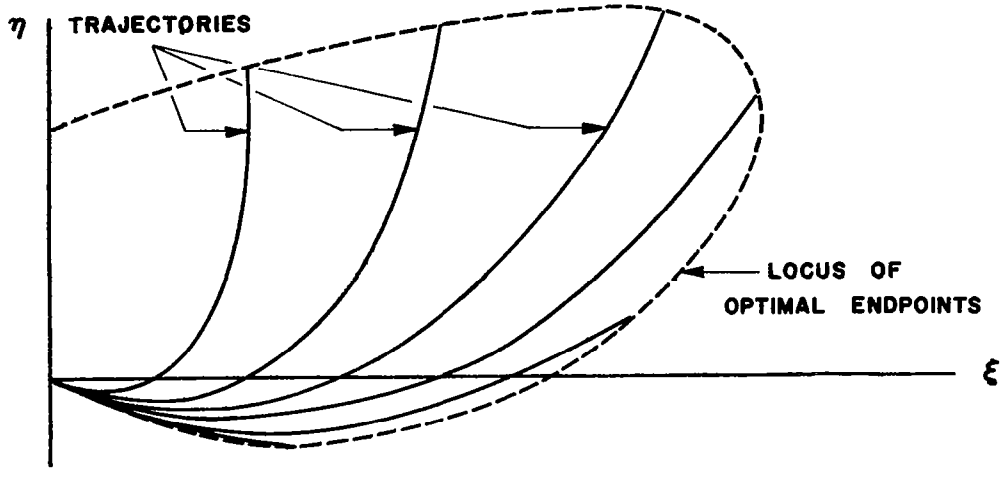

FIGURE 4.1 - GENERATING THE LOCUS OF OPTIMAL ENDPOINTS

If this process is repeated for several different values of the initial flight path angle, the ξ - η plane becomes "flooded" with optimal trajectories and their corresponding loci of optimal endpoints (for example see Figure 4.2). The trajectories corresponding to the various values of γ_1 and λ_ξ may cross, but the loci of optimal endpoints for a given aircraft are non-intersecting. Such plots of the loci of optimal endpoints rather than the trajectories themselves more clearly summarize the results of the analysis.

Computer Results

Cases to be studied. - It was shown in Section III that no discontinuous solutions are obtained when the thrust to weight ratio of the model aircraft is greater than 1.5. This thrust to weight ratio represents a borderline case. For values of the thrust to weight ratio greater than 1.5, every point in ξ - η space can be reached with a continuous solution. Examples of this situation are contained in Figures 4.8 and 4.11. These figures show that the entire ξ - η space may be filled with optimal trajectories for an aircraft with a thrust to weight ratio of 1.8. For values of the thrust to weight ratio less than of 1.5, both continuous and discontinuous solutions are needed to reach every point in ξ - η space. Examples of this situation for a thrust to weight ratio of 0.5 are shown in Figures 4.2 and 4.5. Only the endpoints obtainable with continuous solutions are shown in these figures. The discontinuous solutions which are not shown can be easily computed as previously discussed in Section III. The boundary line between continuous and discontinuous solutions shown in these figures is identical with the boundary as computed in Section III.

It is also shown in Section III that when $u_1 < u_q$, the initial vertical arc was a diving one and when $u_1 > u_q$, the initial vertical arc was a climbing one. A similar effect is also found for the continuous solutions. In order to illustrate the various points of interest pertaining to the continuous solutions, four cases $T/W < 1.5$, $u_1 < u_q$; $T/W < 1.5$, $u_1 > u_q$; $T/W > 1.5$, $u_1 < u_q$; $T/W > 1.5$, $u_1 > u_q$ were examined in detail and the results are presented in Figures 4.2-4.13.

The significance of λ_ξ. - The form of an optimal solution is very sensitive to the parameter λ_ξ. Preliminary consideration of its effect on the solution will aid in comprehending the results. The value of λ_ξ which will yield a solution is always greater than zero but less than $\cos \gamma_1/u_1$ for trajectories proceeding to the right. If λ_ξ is set at a value greater than $\cos \gamma_1/u_1$ the resultant trajectory will ultimately proceed to a terminal dive with no chance of satisfying the endpoint condition, $\lambda_{u2} = 0$. A plot of $\cos \gamma_1/u_1$ for each case is given in Figures 4.3, 4.6, 4.9 and 4.12.

For values of λ_ξ less than $\cos \gamma_1/u_1$ but in the neighborhood of this value, the resultant trajectory is short with a shape that is similar to the initial portion of the locus of optimal endpoints corresponding to the same initial angle. This effect is illustrated in Figures 4.4, 4.7, 4,10 and 4.13 for some typical "short" trajectories. In all cases the length of the trajectory will increase as λ_ξ is decreased from the value $\cos \gamma_1/u_1$. "Long" trajectories

in each case are characterized by a portion of the trajectory being flown in a nearly steady manner. During this portion of the trajectory the slope of the flight path nearly coincides with the linear portion of the corresponding locus (see Figures 4.4, 4.7, 4.10 and 4.13).

In cases when $u_1 > u_q$ the length of the trajectory increases without bound as λ_ξ approaches some fixed number greater than zero. For example, as shown in Figure 4.6 for a trajectory with an initial angle of 0^o and in Figure 4.12 for a trajectory with an initial angle of 30^o, λ_ξ in the neighborhood of point A correspond to the short trajectories shown in Figures 4.7 and 4.13. As the values of λ_ξ approach the point B the length of the trajectories increase without bound to infinity. This effect can be visualized from Figures 4.7 and 4.13. Thus as long as $u_1 > u_q$, the entire spectrum of continuous trajectories are obtained by continually varying λ_ξ from its maximum value of $\cos \gamma_1/u_1$ to some fixed value of $\lambda_\xi > 0$ (point B) for each initial value of γ_1 between $\gamma_1 = \pm 90^o$.

In cases where $u_1 < u_q$ a different phenomena takes place. The locus curves double back on themselves as λ_ξ is decreased from the value $\cos \gamma_1/u_1$ (see Figures 4.2 and 4.8). These curves double back in two distinctly different ways. For example as shown in Figures 4.3 and 4.9 a trajectory with an initial flight path angle γ_1 such that λ_ξ may be chosen freely between the values of $\cos \gamma_1/u_1$ and zero (outside the forbidden zone as illustrated by the line ABC for the $\gamma_1 = -20^o$ case) the resultant trajectory shown in Figure 4.10 increases in length as λ_ξ decreases from its maximum value until the value of λ_ξ corresponding to point B Figures 4.3 and 4.9 is obtained. As λ_ξ is further decreased from the point B the trajectories decrease in length approaching a vertical trajectory of finite length as λ_ξ approaches zero. These latter "zooming" trajectories are illustrated in Figure 4.10.

For a trajectory with an initial flight path angle such that λ_ξ may not be chosen freely between the values of $\cos \gamma_1/u_1$ and zero without intersecting the forbidden zone (illustrated by the line DEFG in Figures 4.3 and 4.9) the resultant trajectory increases in length without bound as λ_ξ decreases from its maximum value to the value at the point E. For values of λ_ξ between the points E and F the resultant trajectory will ultimately proceed to a terminal dive with no chance of satisfying the endpoint condition $\lambda_{uf} = 0$. However, for values of λ_ξ between values corresponding to the point F and zero, the resultant trajectories decrease in length (from infinity) and approach a vertical trajectory of finite length as λ_ξ approaches zero (see Figure 4.4).

The continuous vertical trajectory corresponding to $\lambda_\xi = 0$ is the same for all initial flight path angles γ_1 with the same given initial velocity. This situation occurs by virtue of the fact that as λ_ξ approaches zero, $\dot{\gamma}$ approaches a unit impulse whose magnitude is such that vertical flight is obtained.

Trajectories with $T/W < 1.5$, $u_1 < u_q$. - The loci of optimal endpoints shown in Figure 4.2 were obtained by using the methods outlined previously. These results are typical for $T/W < 1.5$ and $u_1 < u_q$. Specifically these curves are computed for an aircraft with $T/W = .5$, $u_1 = 1.6$ and $u_q = 1.82$.

The majority of points in the ξ - η plane are reached optimally by following a trajectory which dives initially. Only those points which are enclosed in the area bounded by the zero degree locus and the η axis are reached optimally by following a trajectory which climbs initially. These results are consistent with the nature of the discontinuous solutions. These solutions were characterized by starting with a vertical dive, followed by a steady climb, and then a vertical climb. This same order of events becomes characteristic of the continuous solutions if the trajectories are sufficiently long. For example in Figure 4.4 the typical "long" trajectories are characterized by an initial dive which smoothly transforms into a steady trajectory with a slope approximately equal to the corresponding locus line. This steady portion of the trajectory then smoothly transforms into a climb as the final endpoint is approached. Trajectories with endpoints on the upper branch of the loci curves which extend to infinity correspond most markedly to the discontinuous trajectories discussed in Section III. As was the case with the discontinuous trajectories, these continuous trajectories dive initially to pick up a speed near u_q before starting on the optimum steady climb.

A boundary between continuous and discontinuous solutions is drawn and labeled in Figure 4.2. Equation (3.11) was used to determine the slope of the boundary and equations (3.44) and (3.48) were used to determine the η intercept point of the boundary. It is noted that continuous solutions with initial flight path angles approaching -90° generate loci of optimal endpoints which closely follow this boundary. In the limit, this boundary corresponds to the -90° case. Thus above this line solutions are all discontinuous while below this line the solutions are entirely continuous. Trajectories with endpoints in the neighborhood of the boundary between continuous and discontinuous solutions and the η axis execute a very strong pull-up during the initial portion of the trajectory. These have been classed as "zooming" trajectories and a typical example is shown in Figure 4.4.

It is evident that all of the locus curves intersect the η-axis at a given critical point. To optimally reach points directly below this critical point, an aircraft must climb vertically directly to the endpoint. However, to reach point directly above the critical point, the aircraft must dive vertically until it has attained the velocity u_q. Then the aircraft must climb vertically to the endpoint. The locus of optimal endpoints corresponding to the -90° case is comprised of the boundary locus together with that portion of the η-axis between the critical point and the boundary locus.

Trajectories with $T/W < 1.5$, $u_1 > u_q$. - The optimal results shown in Figure 4.5 are typical for $T/W < 1.5$ and $u_1 < u_q$. Specifically these curves correspond to an aircraft with $T/W = .5$, $u_1 = 2$ and $u_q = 1.82$. For any given initial flight path angle the locus curves are generated by varying the parameter λ_ξ between $\cos \gamma_1/u_1$ and a constant > 0 as shown in Figure 4.6.

Unlike the previous example the locus of optimal endpoints do not double back but rather asymptotically approach a straight line which extends to infinity.

The value of the multiplier λ_ξ also asymptotically approaches some fixed value as an endpoint is moved further and further along a given locus.

The boundary between continuous and discontinuous solutions corresponds to the $\gamma_1 = +90^o$ case and is identical with the discontinuous boundary locus obtained by using equations (3.11), (3.45) and (3.49). Above this boundary, solutions are discontinuous and below this boundary solutions are continuous. It is noted in this case that the $\xi - \eta$ plane is more or less divided equally between trajectories which are initiated with a dive and trajectories which are initiated with a climb. Points above the $\gamma_1 = 0^o$ locus are obtained by following a trajectory which climbs initially and points below the $\gamma_1 = 0^o$ locus are obtained by following a trajectory which dives initially. All the discontinuous trajectories are reached by initially climbing vertically as was shown in Section III.

As shown in Figure 4.7 the actual trajectories at a distance from the origin, below the $\gamma_1 = 0^o$ locus are characterized by an initial dive followed by a steady portion of the trajectory which is followed by a climb. Above the $\gamma_1 = 0^o$ locus the trajectories are characterized by an initial climb followed by a steady portion followed by a final climb.

Trajectories with $T/W > 1.5$, $u_1 < u_q$. - The locus of optimal endpoints shown in Figure 4.8 are typical for $T/W > 1.5$ and $u_1 < u_q$. Specifically these curves were computed for an aircraft with $T/W = 1.8$, $u_1 = 2$ and $u_q = 3.46$. The predicted difference between the results of this case and the previous two cases in which T/W was less than 1.5 is that the $\xi - \eta$ plane is completely filled with continuous optimal trajectories. The form of the solutions are similar to the previous case when $u_1 < u_q$ (T/W =.5). The loci of optimal endpoints are observed to double back on themselves. Only a small portion of the $\xi - \eta$ plane may be reached by initially climbing, namely those points which are endlosed in the area bounded by the $\gamma_1 = 0^o$ locus and the η-axis. All other points in $\xi - \eta$ space are reached by initially diving.

Trajectories to high altitudes near the η axis start with a steep initial dive and then execute a very strong pullup to a steep steady climbing trajectory. This manouver picks up a velocity near u_q which is optimum for climbing.

It is noted that the locus curves corresponding to steep initial dives followed by climbs to high altitude (γ_1 = -30, -45, -60 and -80) are approximately straight lines intersecting the η-axis at the point $\eta = 7.25$. This critical point divides trajectories with endpoints directly overhead into two categories. In order to reach points from $\eta = 0$ to the critical η value the aircraft must climb vertically directly to the endpoint. However, to reach a point directly overhead which is above the critical η value, the aircraft must dive vertically until it attains a velocity of u_q from which point it climbs vertically to the endpoint. For this special case of endpoints directly overhead the continuous solution degenerates into a discontinuous solution.

Trajectories with $T/W > 1.5$, $u_1 > u_q$. - The loci of optimal endpoints shown in Figure 4.11 are typical for $T/W > 1.5$ and $u_1 > u_q$. Specifically these curves correspond to an aircraft with $T/W = 1.8$, $u_1 = 4$ and $u_q = 3.46$. With $u_1 > u_q$, the loci of optimal endpoints do not double back on themselves

but rather form nearly straight lines which in all cases extend to infinity.

Because of the high T/W ratio the loci have very little curvature and are approximately straight lines passing through the origin. From Figure 4.13 it is evident that the actual trajectories are also nearly straight lines and practically coincide with their corresponding loci. Thus, as might be expected the case of very high T/W with $u_1 > u_q$ an aircraft can optimally reach any point in $\xi - \eta$ space by flying almost directly to the endpoint along a straight line.

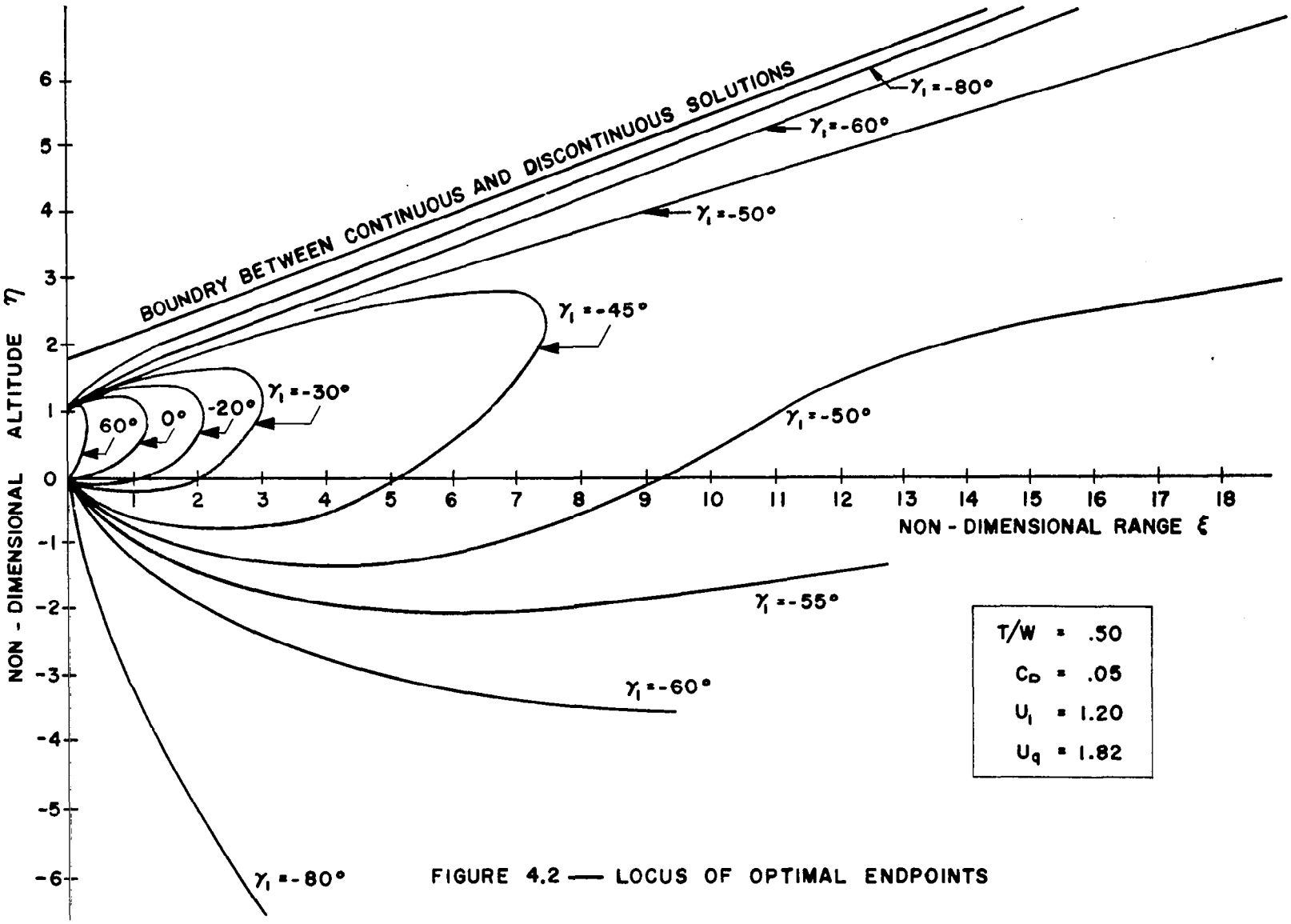

FIGURE 4.2 — LOCUS OF OPTIMAL ENDPOINTS

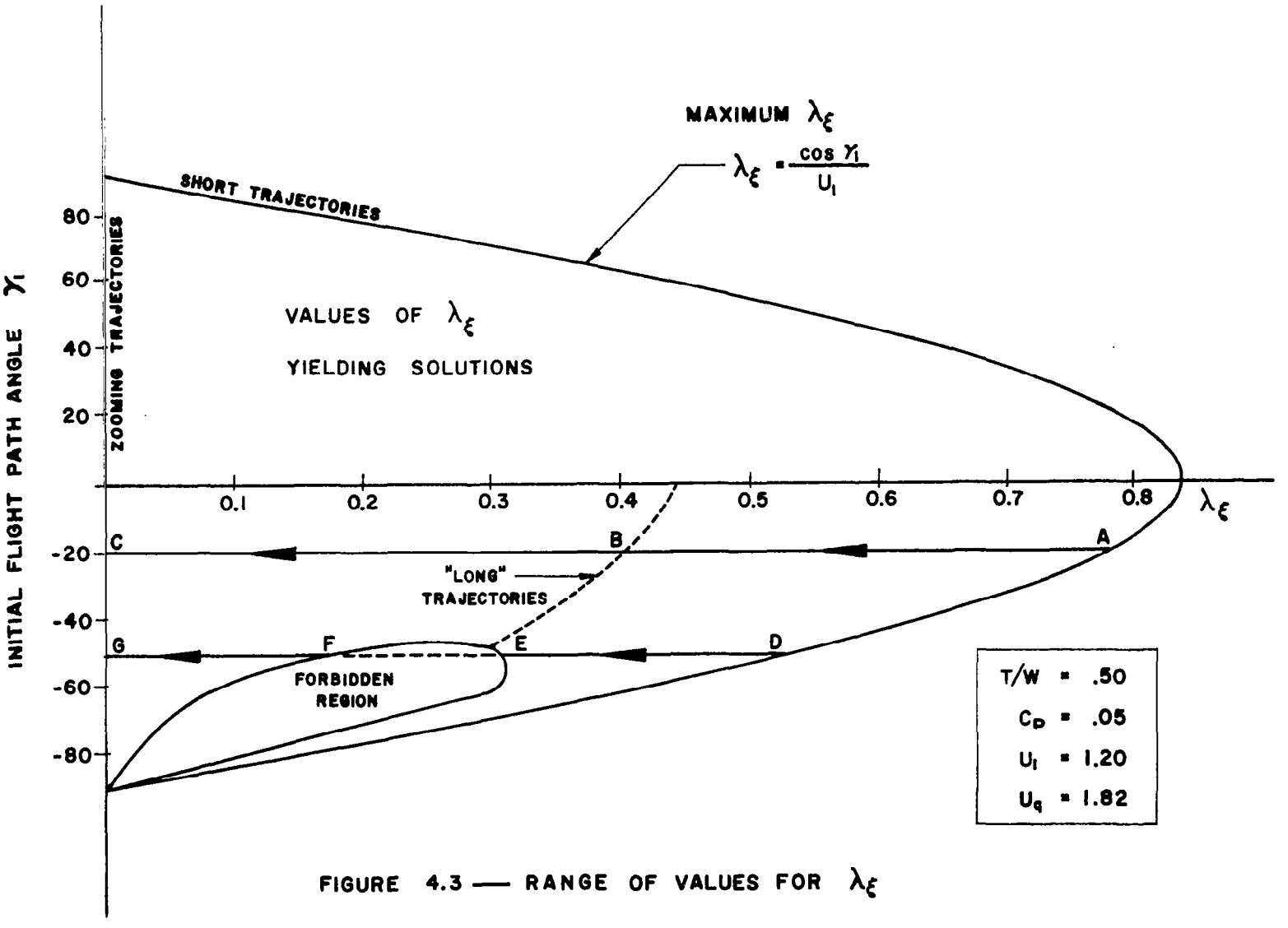

FIGURE 4.3 — RANGE OF VALUES FOR λ_ξ

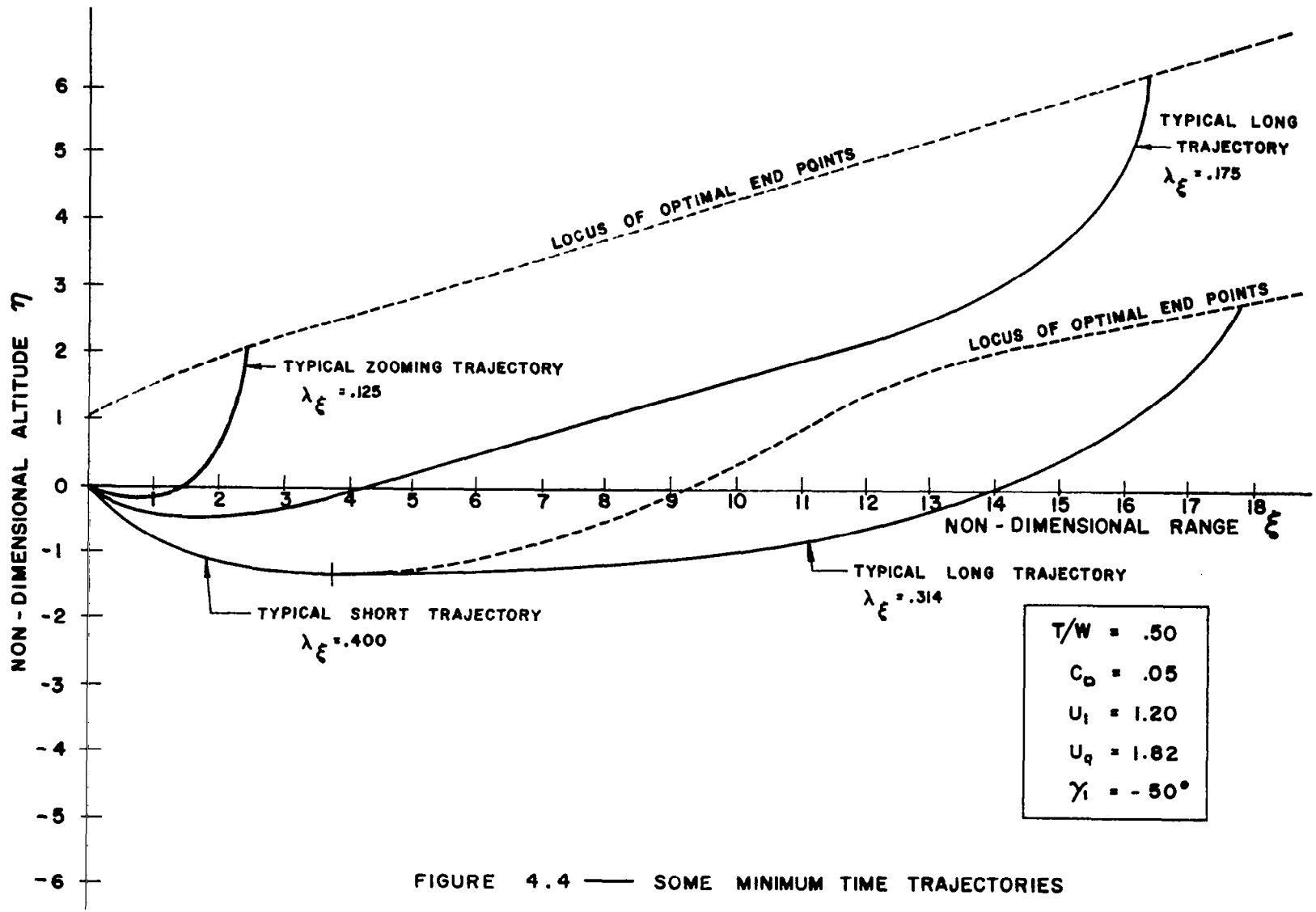

FIGURE 4.4 —— SOME MINIMUM TIME TRAJECTORIES

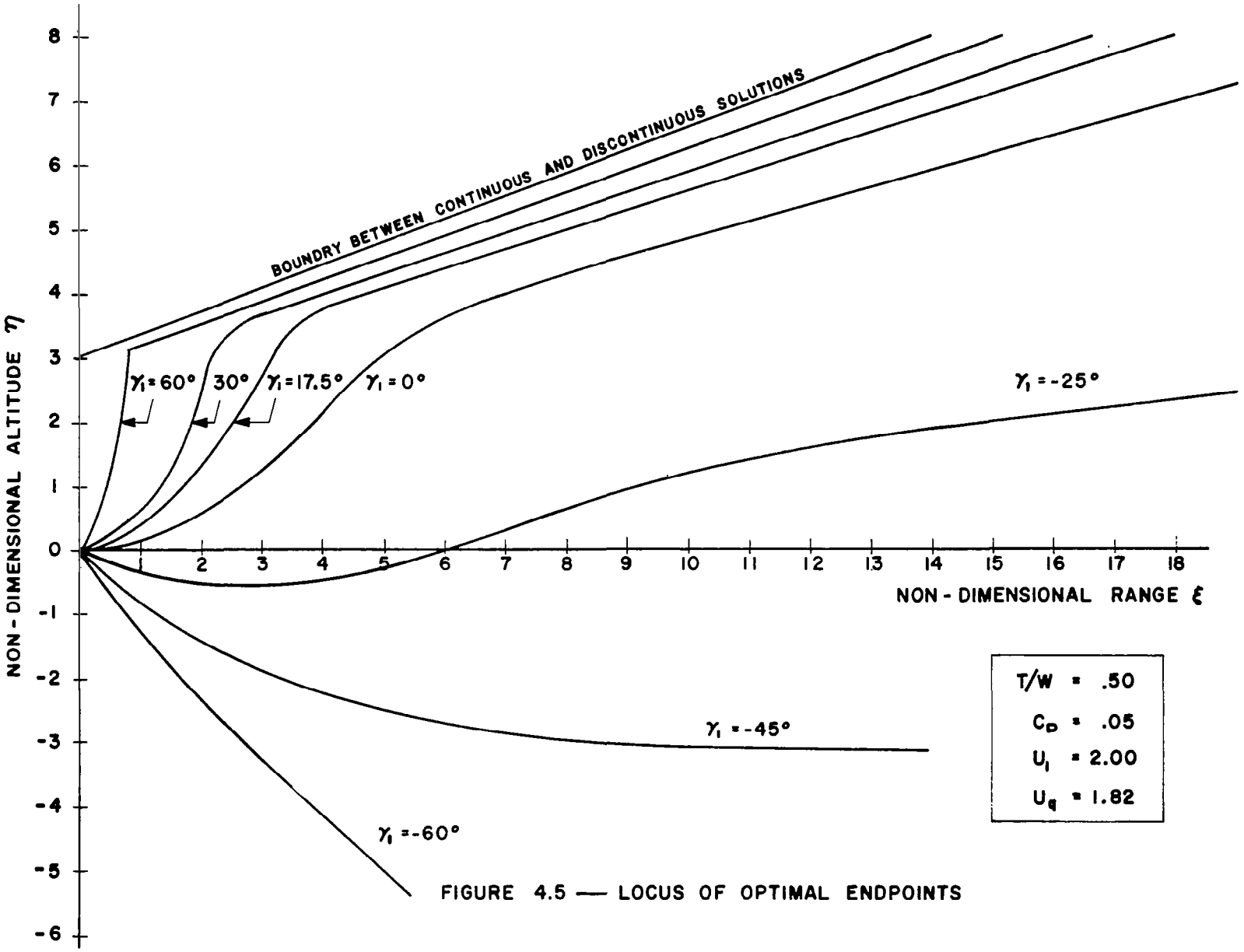

FIGURE 4.5 — LOCUS OF OPTIMAL ENDPOINTS

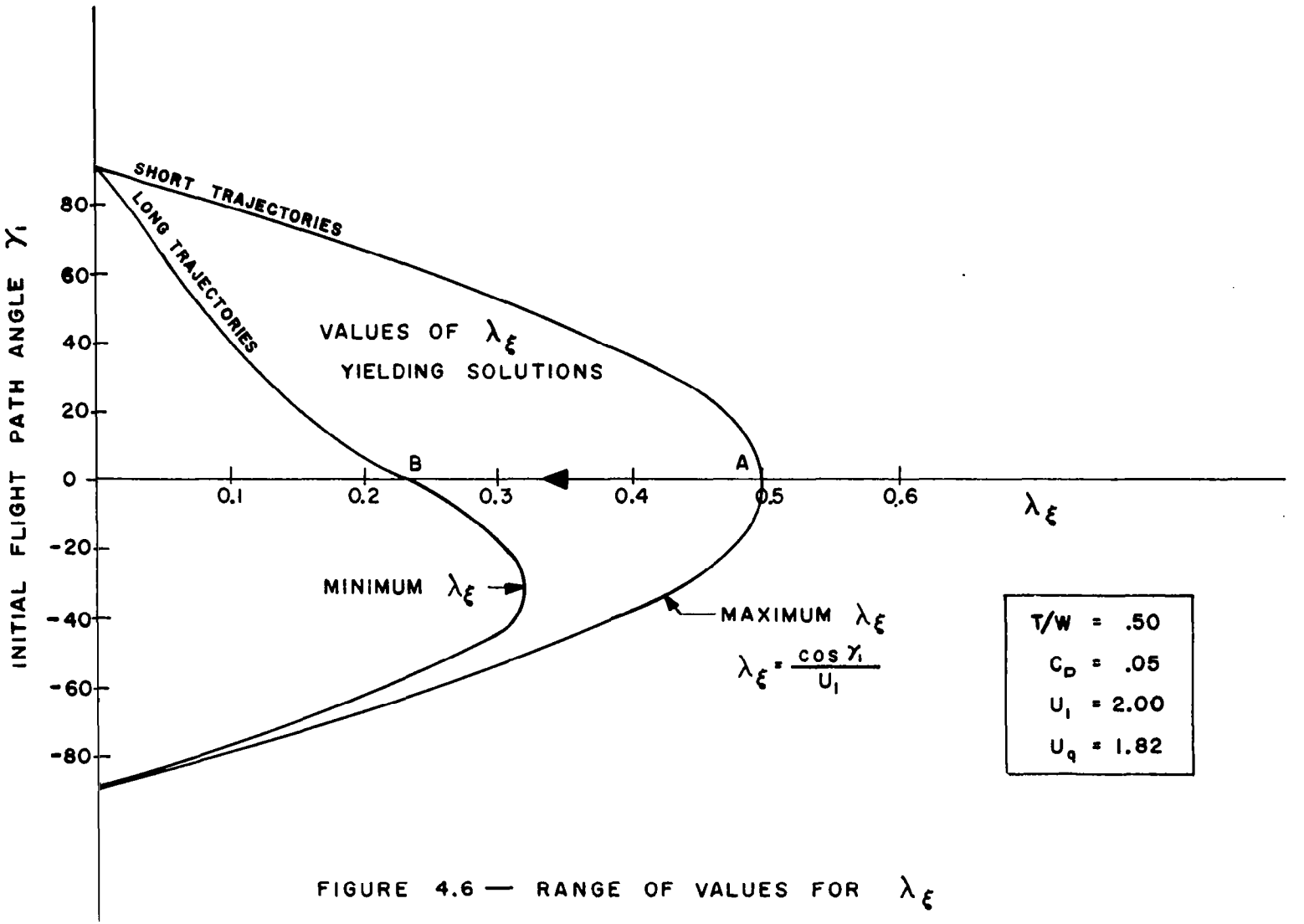

FIGURE 4.6 — RANGE OF VALUES FOR λ_ξ

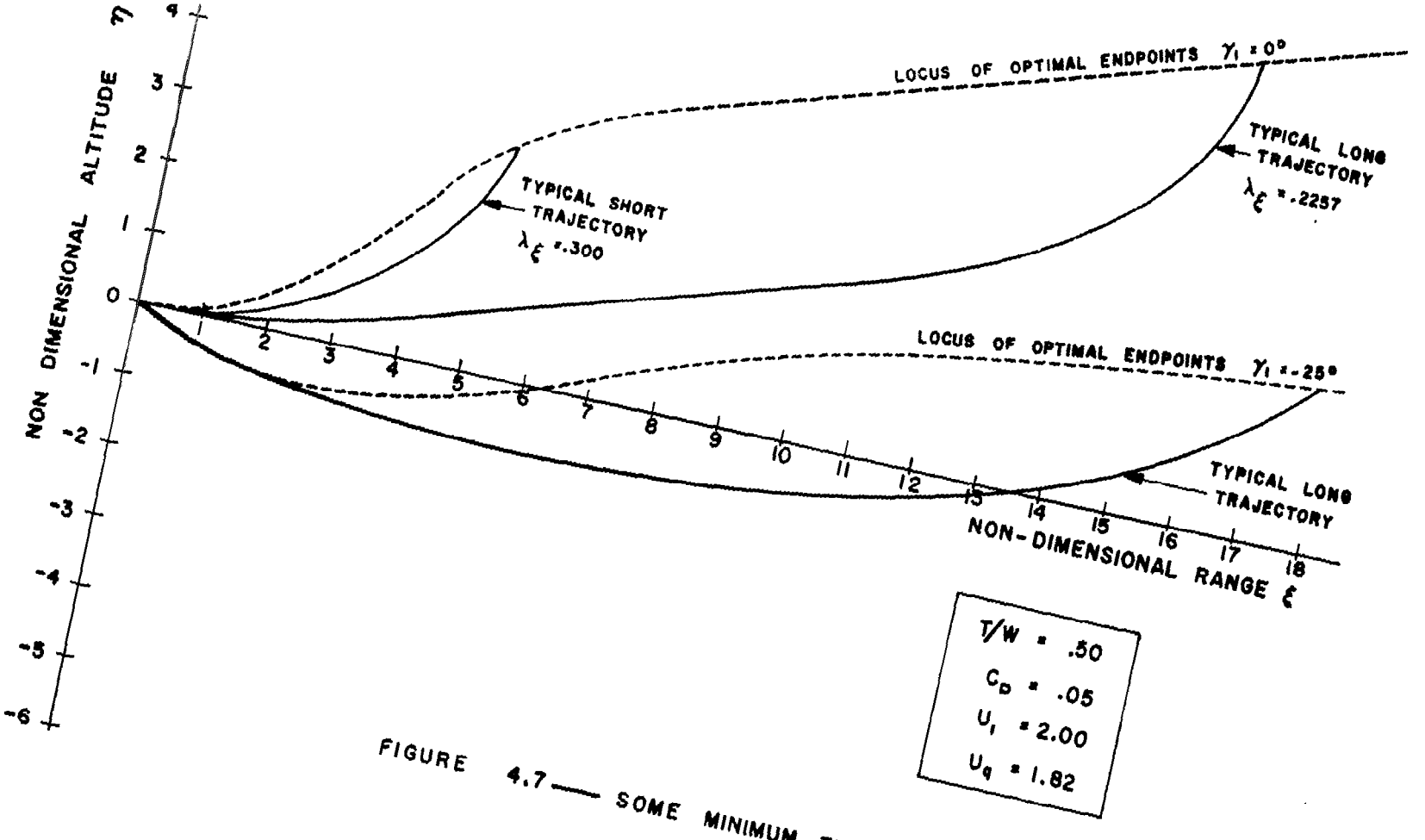

FIGURE 4.7 — SOME MINIMUM TIME TRAJECTORIES

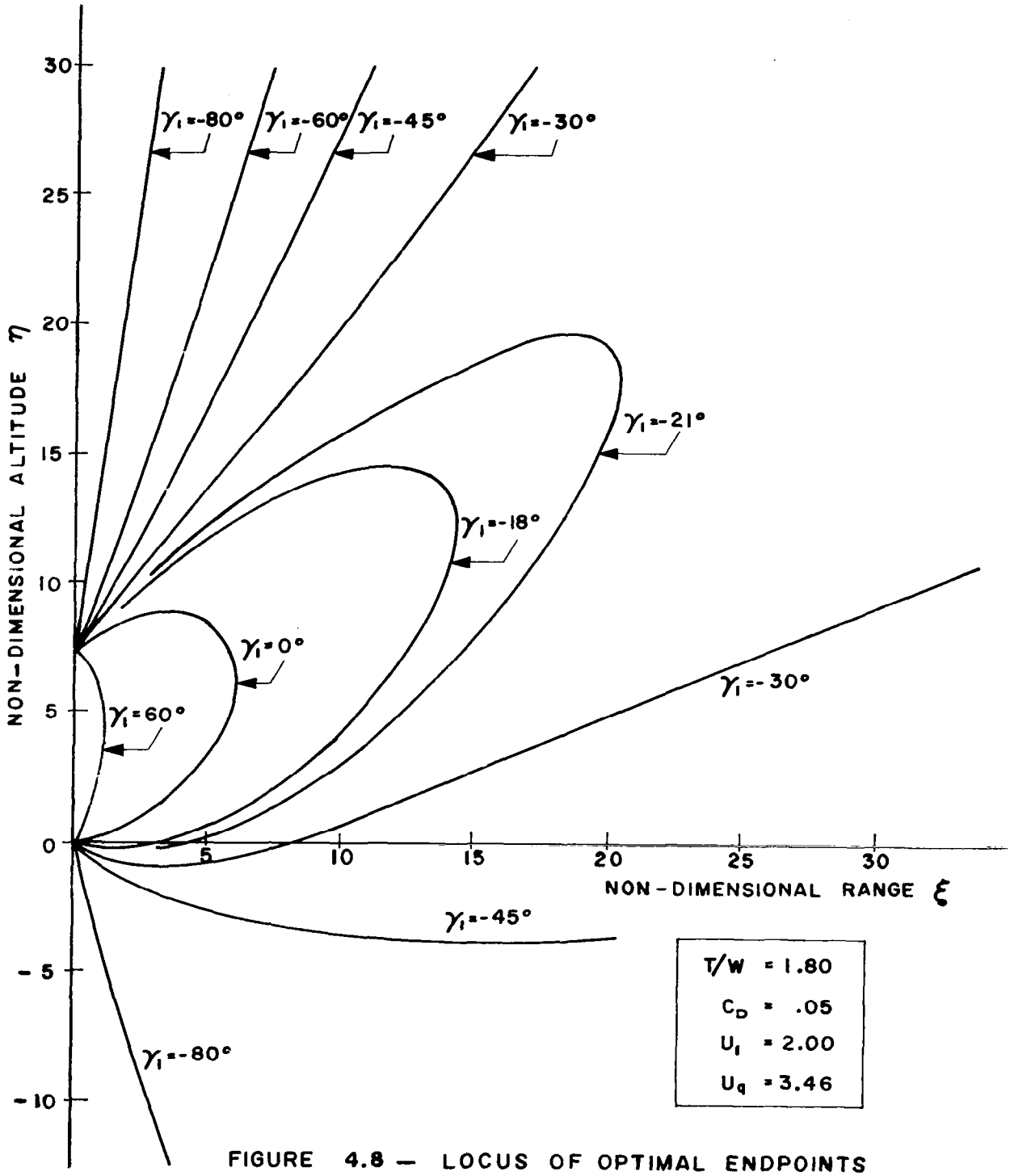

FIGURE 4.8 — LOCUS OF OPTIMAL ENDPOINTS

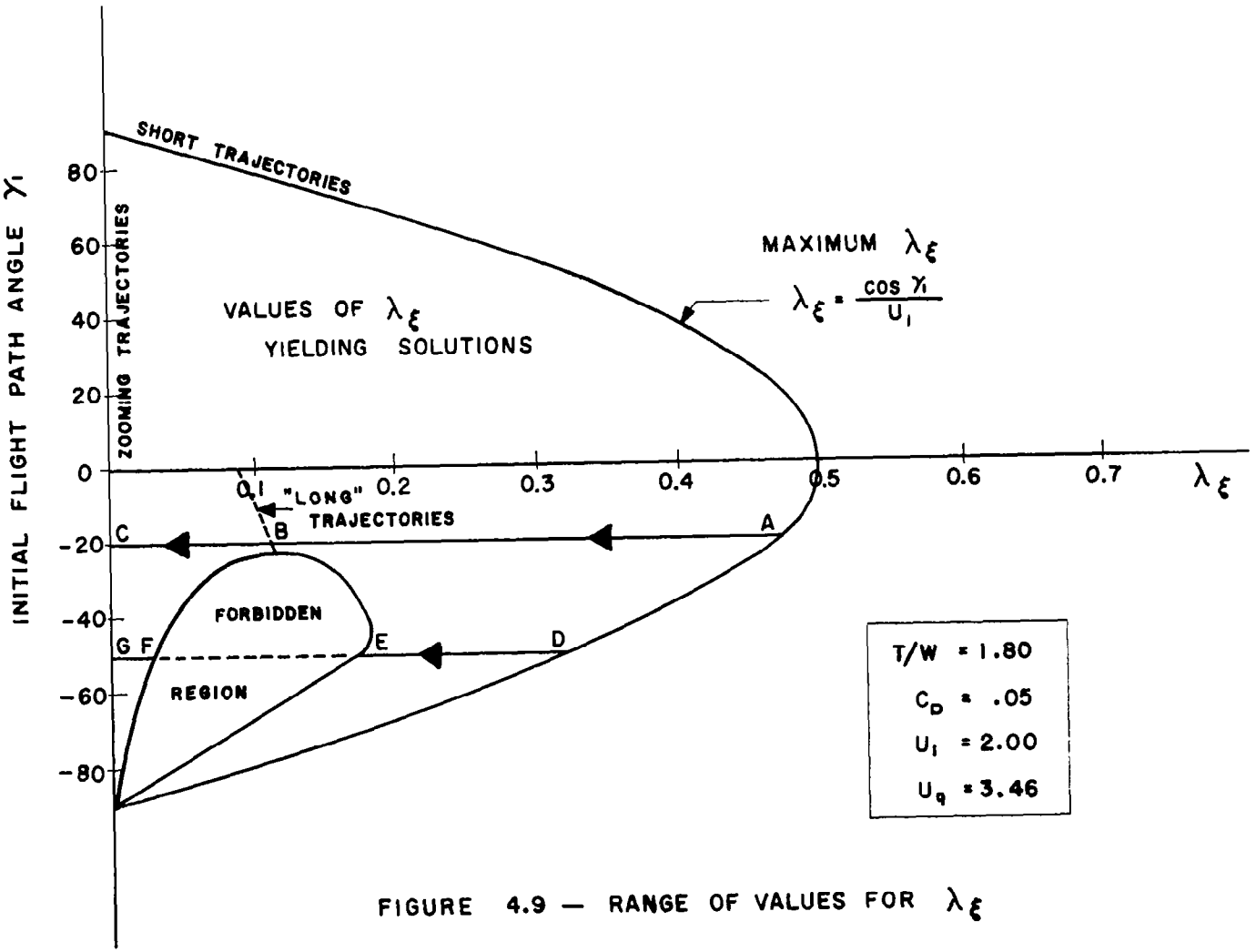

FIGURE 4.9 — RANGE OF VALUES FOR λ_ξ

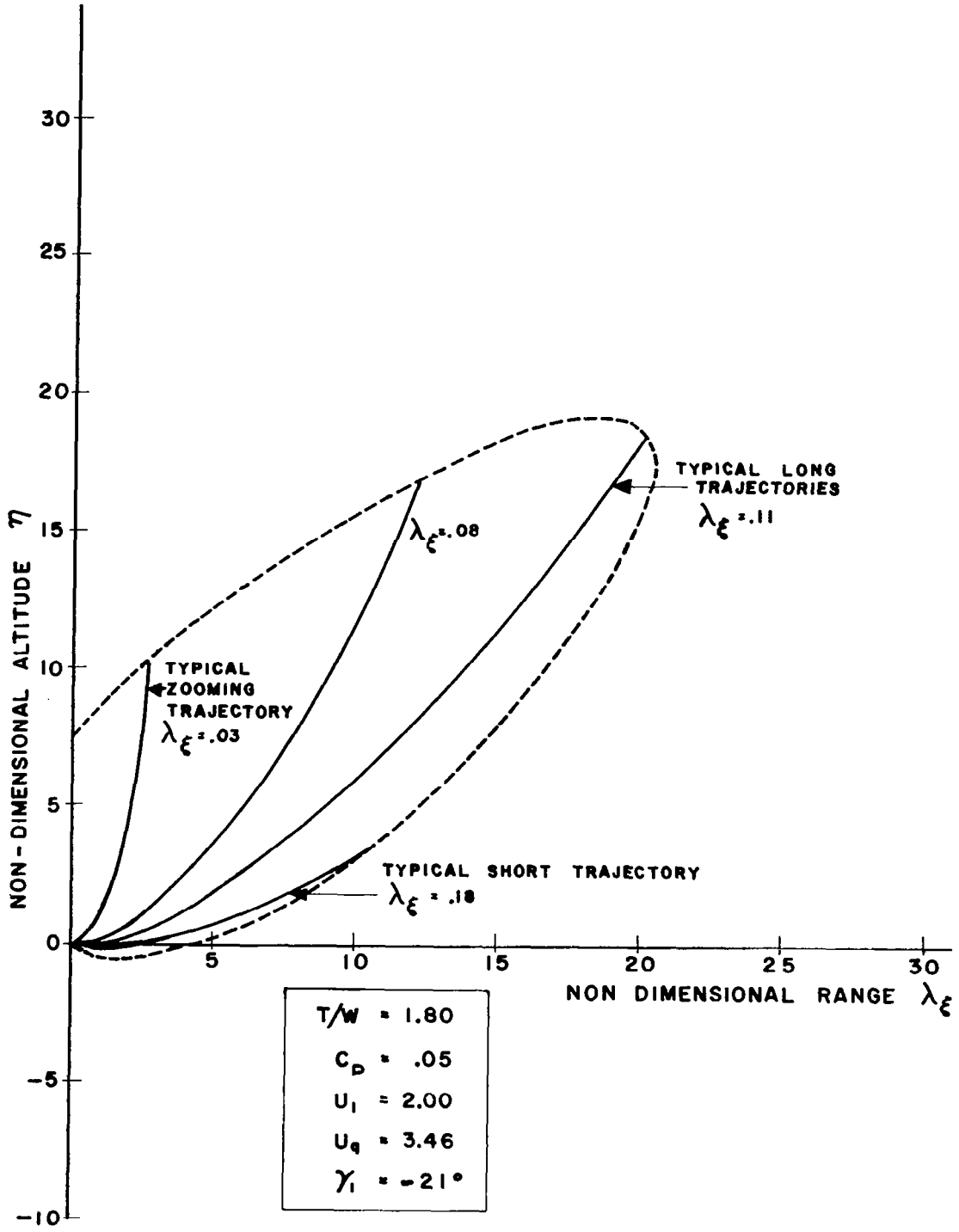

FIGURE 4.10 — SOME MINIMUM TIME TRAJECTORIES

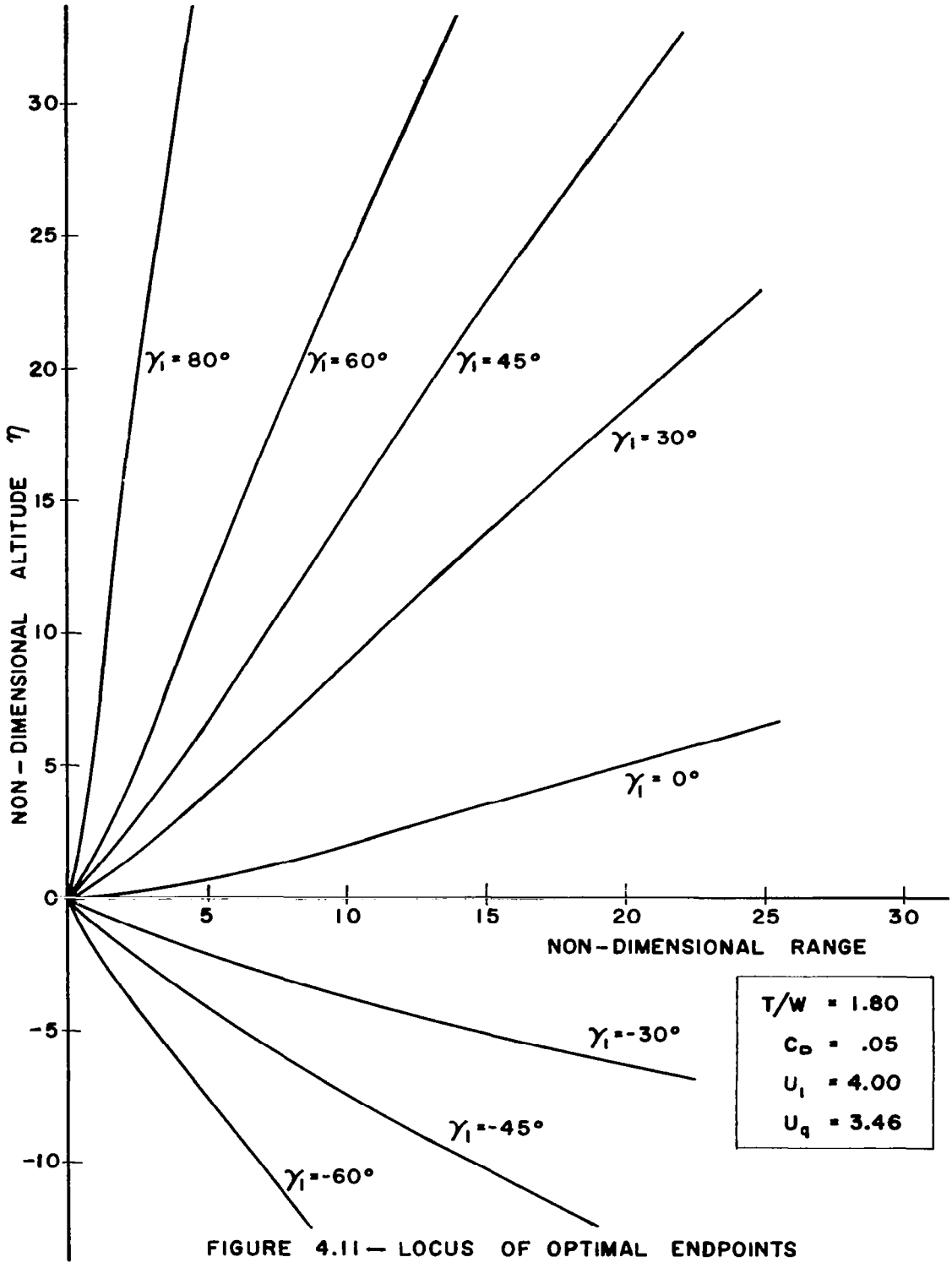

FIGURE 4.11 — LOCUS OF OPTIMAL ENDPOINTS

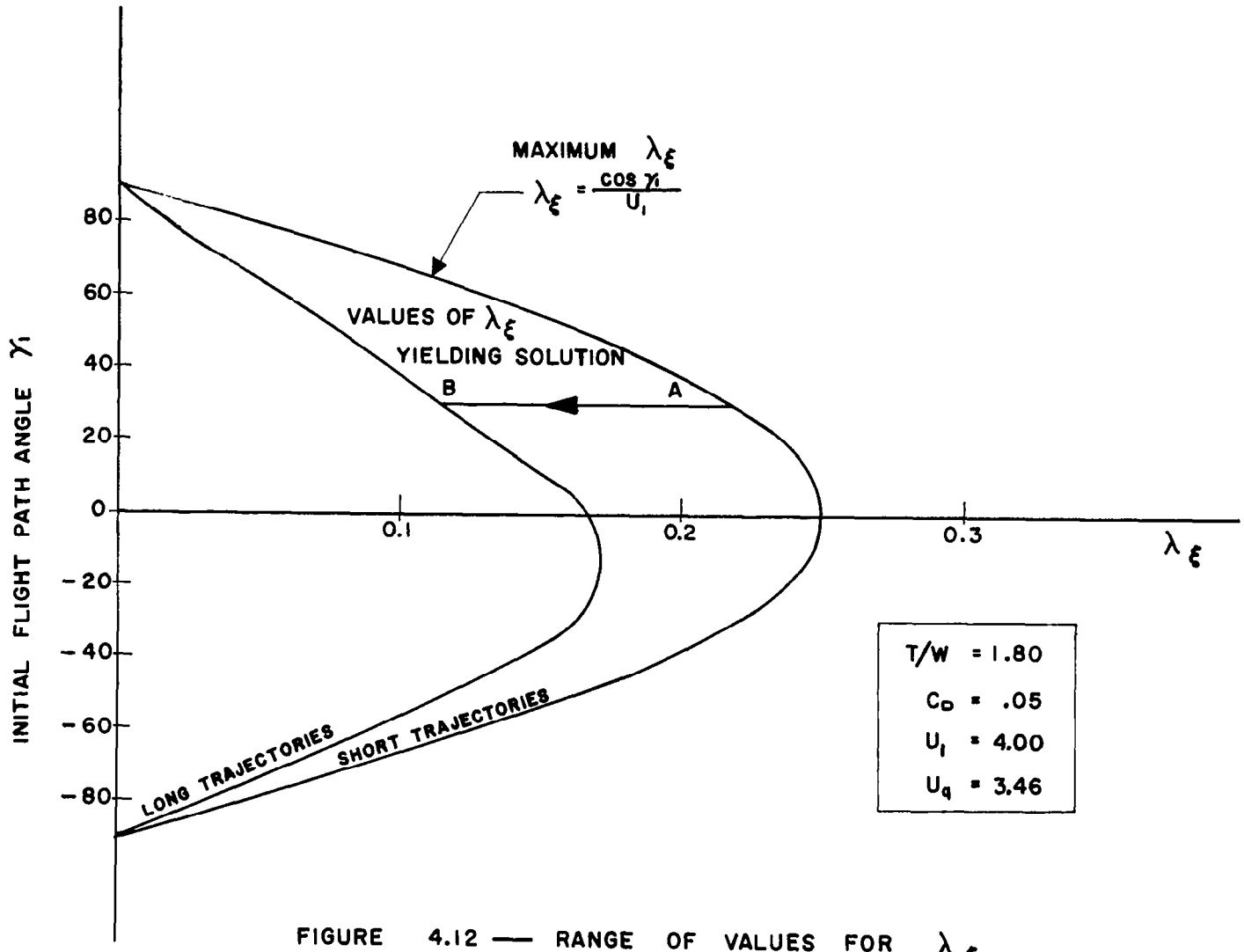

FIGURE 4.12 — RANGE OF VALUES FOR λ_ξ

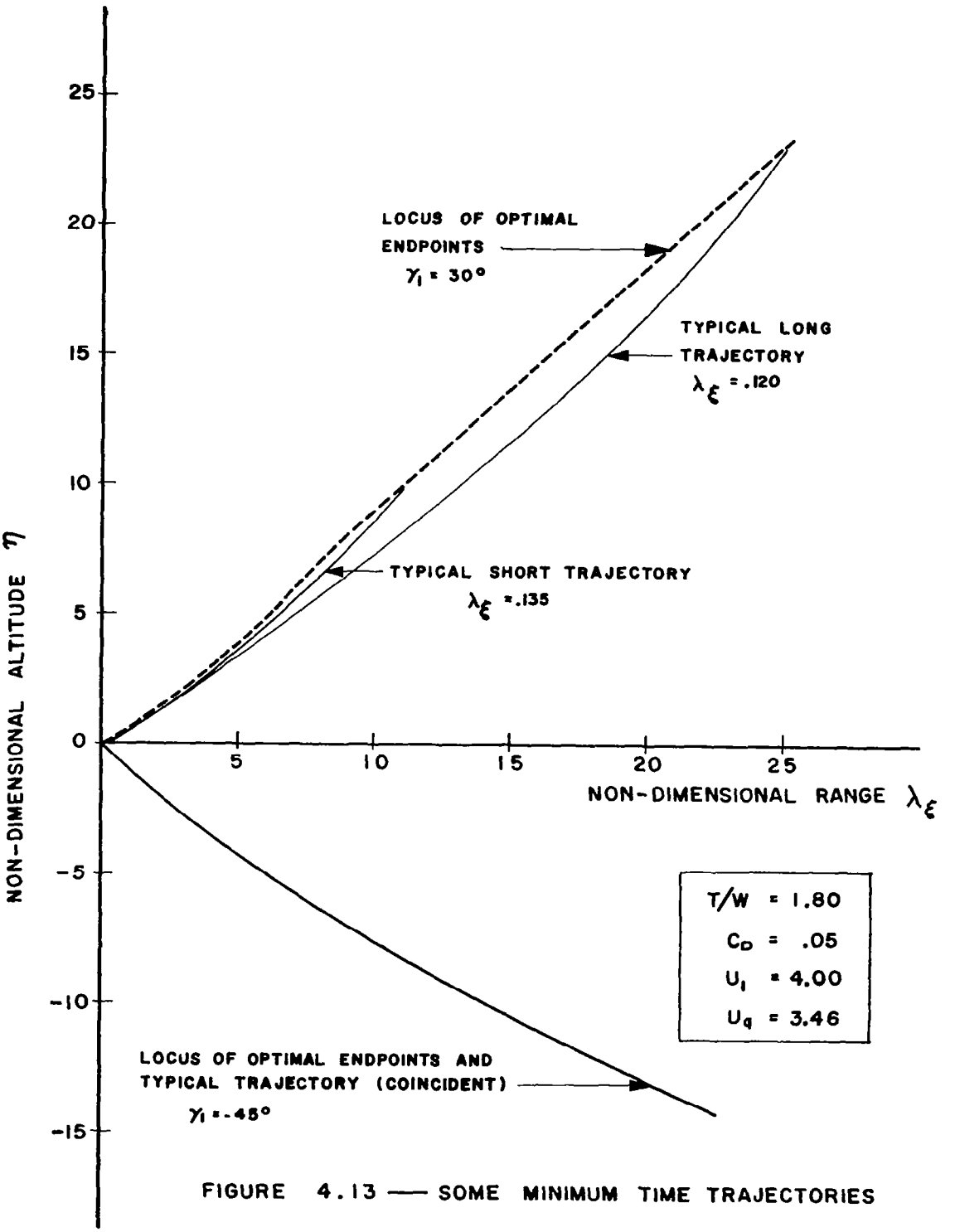

FIGURE 4.13 — SOME MINIMUM TIME TRAJECTORIES

SECTION V

DISCUSSION AND CONCLUSIONS

The analysis of Section II was restricted to two dimensional motion of an aircraft in a uniform gravitational field with thrust and drag given as specified functions of altitude and velocity. Under these conditions, theoretical considerations show that the form of a minimum time trajectory between two points in range-altitude space will in general fall into one of two distinctively different categories. Depending upon the location of the endpoint, the trajectory will either be continuous with the flight path angle given by one control law, or the trajectory will be discontinuous with the flight path angle given by yet another control law. It was shown in Sections III and IV for a constant thrust aircraft with drag proportional to velocity squared that the discontinuous solutions are not obtained unless the thrust to weight ratio of the aircraft is less than three halves. Under this circumstance, part of the range-altitude space is filled with continuous solutions with a common boundary between the two regions.

Both the continuous and discontinuous solutions are characterized by the relation of u_1 to u_q. The most evident effect of this relation on the discontinuous solutions is that if $u_1 < u_q$ then the initial subarc trajectory is a vertical dive and if $u_1 > u_q$ then the initial subarc trajectory is a vertical climb. The most notable effect on the continuous solutions is that if $u_1 < u_q$ then the locus curves as shown in Figures 4.2 and 4.8 double back on themselves. This effect is also illustrated in Figure 5.1 where $u_1 = u_q \pm \epsilon$. With $u_1 = u_q + \epsilon$ the locus curves extend to the right to infinity and with $u_1 = u_q - \epsilon$ the locus curves double back. This effect is explained on the basis that if $u_1 < u_q$ the boundary between continuous and discontinuous solutions must be obtained as $\gamma_1 \longrightarrow -90^\circ$ (an initial vertical dive) whereas if $u_1 > u_q$ this boundary must be obtained as $\gamma_1 \longrightarrow +90^\circ$ (an initial vertical climb).

Even though the model aircraft used in generating the solutions in Sections III and IV was elemental in nature, considerable difficulty would be experienced in general if a standard trial and error technique were used to solve the optimizing equations rather than the flooding technique used here. A trial and error method which involves the adjustments of the initial Lagrange multipliers in the Euler equations to meet specified end conditions will encounter convergence difficulties. This is partially because the influence of the Lagrange multipliers λ_ξ on the location of the resultant endpoint is highly non linear. For example in the vicinity of points A and D in Figures 4.3 and 4.9 and point A in Figures 4.6 and 4.12 a small change in λ_ξ keeping other quantities constant will result in a relatively small change in the resultant trajectory. However for values of λ_ξ in the vicinity of points E and F in Figure 4.3 and 4.9 and point B in Figures 4.6 and 4.12 a small change in λ_ξ will result in an exceedingly large change in the resultant trajectory. In addition, for the value of $\lambda_\xi = 0$ there are an infinite number of optimal discontinuous trajectories. The degree of difficulty in applying some trial and error technique is a strong function of where the desired endpoint is located.

Only the gross effects of thrust and drag on the form of a minimum time optimal trajectory were considered here with no constraints imposed on the possible aircraft motion. It is interesting to note from Figure 5.2 that the lift coefficients needed to fly all but the zooming type of trajectories are within the capabilities of most high performance aircraft. Certainly the zooming trajectories and discontinuous trajectories presented here can only be approximated in actual practice. If a more realistic model aircraft had been used with constraints imposed on the inertial capabilities of the craft the resultant trajectories would be rounded somewhat from the ones shown here. It has been previously shown by Hong[6] that for the time to climb problem even the introduction of induced drag will eliminate discontinuous solutions.

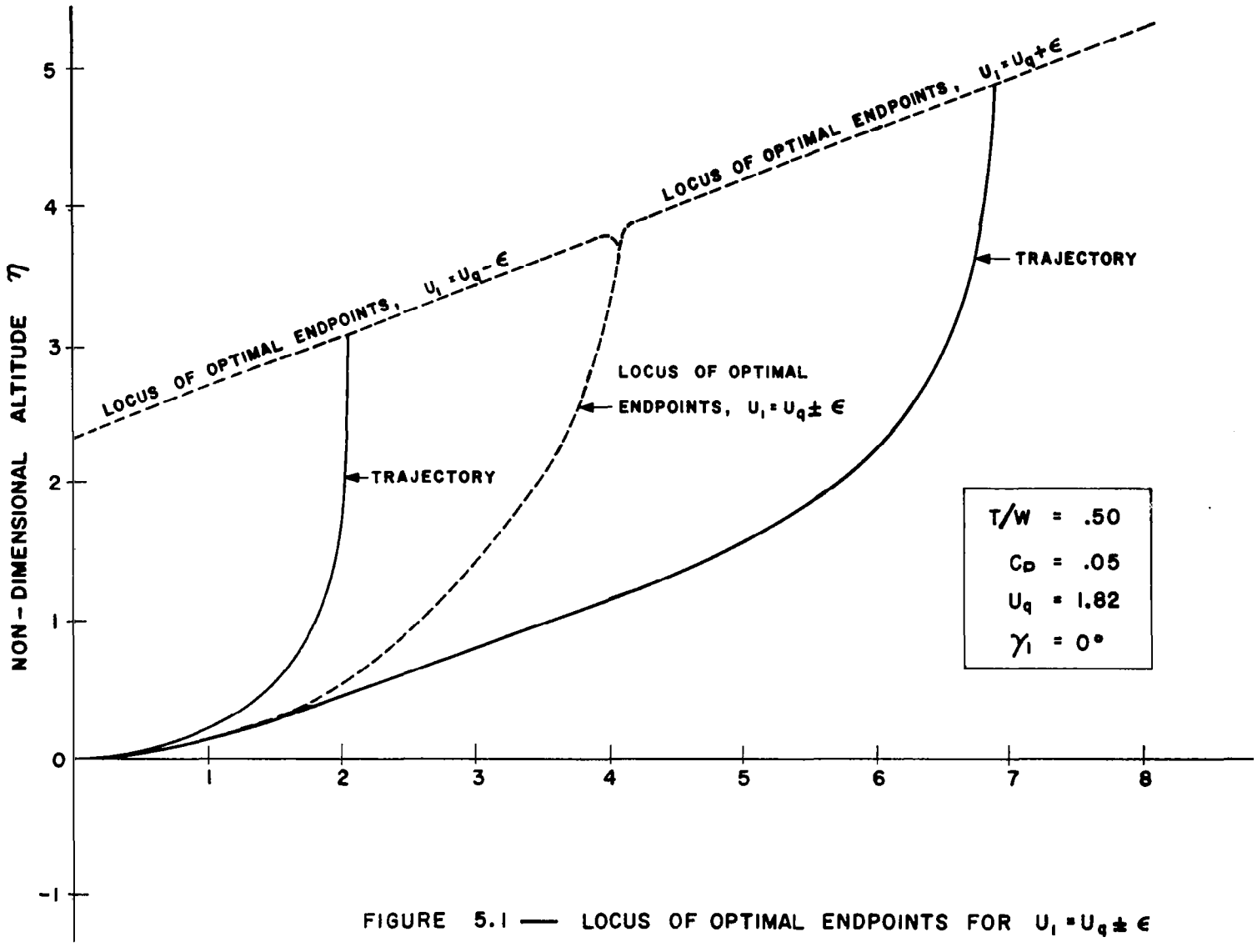

FIGURE 5.1 — LOCUS OF OPTIMAL ENDPOINTS FOR $U_1 = U_q \pm \epsilon$

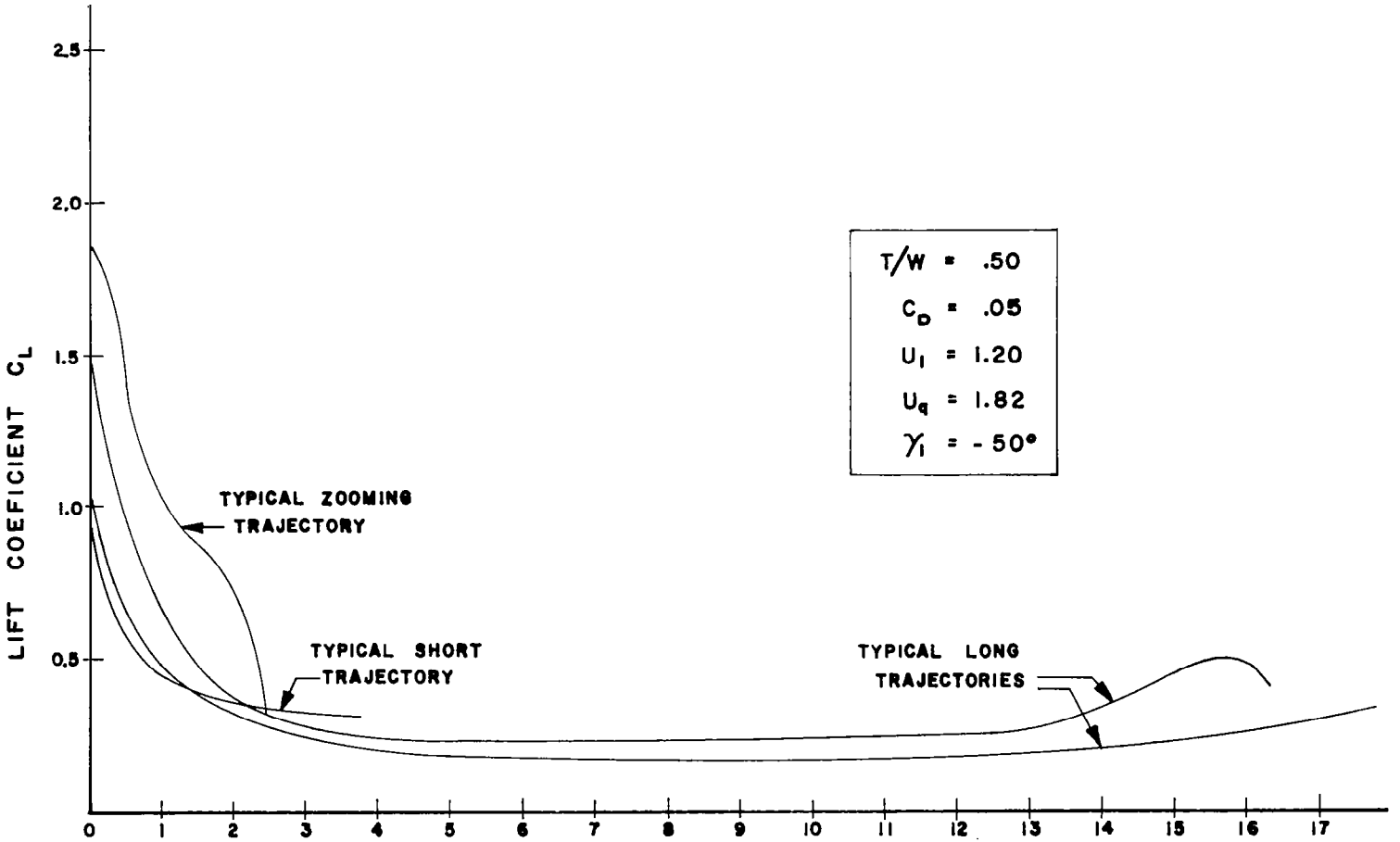

FIGURE 5.2 —— LIFT COEFFICIENT FOR SOME OPTIMAL TRAJECTORIES

REFERENCES

1. Garfinkel, Boris, "Minimal Problems in Airplane Performance," Quarterly of Applied Mathematics Vol. 9, No. 2, 1951.

2. Miele, Angelo, "Optimum Climbing Techniques for a Rocket Powered Aircraft," Jet Propulsion Vol. 25, pp. 385-391, August, 1955.

3. Theodorsen, T., "Optimum Path of an Airplane - Minimum Time to Climb," Journal of the Aerospace Sciences, Vol. 26, pp. 637-624, October, 1959.

4. Heerman, Hugo and Krelsinger, Phil, "The Minimum Time Problem," Journal of the Astronautical Sciences, Winter, 1964.

5. Vincent, T. L., Lutze, F. and Ishihara, T., "Applications of the Calculus of Variations to Aircraft Performance," NASA CR-499, May 1966.

6. Hong, P. E., "An Investigation of Aircraft Flight Paths for Minimum Time to Climb," A Master's Thesis, The University of Arizona, 1965.